STRUCTURE OF A QUASI-PARALLEL, QUASI-LAMINAR BOW SHOCK

by

E. W. Greenstadt[1], C. T. Russell[2], V. Formisano[3], P. C. Hedgecock[4], F. L. Scarf[1], M. Neugebauer[5], and R. E. Holzer[2]

July 1976

NASW-3392

[1]Space Sciences Department, TRW Systems, One Space Park, Redondo Beach, California 90278

[2]Institute of Geophysics and Planetary Physics, University of California, Los Angeles, Los Angeles, California 90024

[3]CNR-LPS Laboratorio Plasma Spazio, P.O. Box N. 27, 00044 Frascati, Italy

[4]Imperial College of Science and Technology, Department of Physics, South Kensington, London S.W. 7, England

[5]Jet Propulsion Laboratory, 4800 Oak Grove Drive, Pasadena, California 91103

Short Title: QUASI-PARALLEL BOW SHOCK

Space Sciences Department
TRW Systems
One Space Park
Redondo Beach, California 90278

STRUCTURE OF A QUASI-PARALLEL, QUASI-LAMINAR BOW SHOCK

ABSTRACT

A thick, quasi-parallel bow shock structure was observed, for $\theta_{NB} \lesssim 10°$, $\beta_i \approx .3$, $M_A \approx 4$, on 14 February 1969, with field and particle detectors of both HEOS 1 and OGO 5. The typical magnetic pulsation structure was at least 1 to 2 R_E thick radially and was accompanied by irregular but distinct (average) plasma distributions characteristic of neither the solar wind nor the magnetosheath. Waves constituting the large pulsations were polarized principally in the plane of the nominal shock, therefore also in the plane perpendicular to the average interplanetary field. The solar wind was relatively unaffected in bulk velocity in the pulsation structure but was moderately thermalized and its spectra showed a high energy tail. There appeared to be a separate "interpulsation" regime occurring between bursts of large amplitude oscillations. This regime was similar to the upstream wave region magnetically, but was characterized by disturbed plasma flux and enhanced noise around the ion plasma frequency. The shock structure appeared to be largely of an oblique, whistler type, probably complicated by counterstreaming high energy protons. Evidence for firehose instability-based structure was weak at best and probably negative.

INTRODUCTION

One of the fundamental structures of collisionless plasma shocks occurs when the angle θ_{nB} between the magnetic field $\underset{\sim}{B}$ in the unshocked upstream plasma and the direction $\underset{\sim}{n}$ of shock propagation is zero, i.e., when $\theta_{nB} \equiv \arccos(\underset{\sim}{n} \cdot \underset{\sim}{B}/|\underset{\sim}{B}|) = 0$. Such a shock is called a parallel shock and has been studied theoretically and numerically by many authors, of whom a few are Kellogg (1964), Kennel & Sagdeev (1967), Biskamp & Welter (1972), Auer & Völk (1973), and Tidman & Krall (1971). In application to space plasmas, a geometrical basis for variable, asymmetric, and parallel features in the bow shock was postulated very early by Kellogg (1962). Indeed, phenomena probably associated with parallel bow shock structure had been the longest recorded, if not the most familiar, shock characteristics since the first penetration of the magnetosheath by Pioneer I in 1958 (Sonett et al., 1959; for a concise summary of the first decade of satellite measurements related to parallel structure see Greenstadt et al, 1970a). Nevertheless, the importance of field orientation to shock phenomenology was not verified observationally or really appreciated until analysis of multiple satellite data was undertaken (Greenstadt et al., 1970a, b; Greenstadt, 1972a). The investigation continues with this study.

The principal advance in geometric studies since 1970 has been the recognition that a distinct and unmistakable set of macrostructural characteristics occur when $\theta_{nB} \lesssim 40\text{-}50°$, quite unlike the variable, but relatively well-ordered shock signatures that occur in both the laboratory and space when $45° \lesssim \theta_{nB} \leq 90°$ (Robson, 1969; Greenstadt et al., 1975; Fairfield and Feldman, 1975). Shocks with θ_{nB} in the range > 0 to $\approx 45°$, i.e., those having "pulsation"

characteristics and upstream waves, have been designated quasi-parallel. This appellation describes their approximate geometry, their unity of appearance, and their separateness from "quasi-perpendicular" shocks ($45° \lesssim \theta_{nB} \lesssim 88°$) while carefully avoiding any implied conclusion that observed features are necessarily identical to those that might be produced under the precise condition $\theta_{nB} = 0$. Theoreticians have generally proposed that phenomena inferred for the $\theta_{nB} = 0$ state could be extended to some $\theta_{nB} \neq 0$, but no firm angular limits to such extrapolations have been determined. In the Discussion section of this paper, we shall question the meaning of exact parallelism in the bow shock, basing our views on the data presented in this communication..

At the same time that geometrically dependent properties of the bow shock have been uncovered, the effects of other parameters of the solar wind plasma on shock structure have also been isolated and investigated. The result has been an empirically-derived scheme of shock classification using ratio of thermal to field pressure β, Mach number M, and θ_{nB}, several versions of which have recently been published (Formisano & Hedgecock, 1973a; Dobrowolny & Formisano, 1973; Formisano, 1974; Greenstadt, 1974). This report describes in detail a quasi-parallel shock encounter lasting about two hours at HEOS 1, somewhat less at OGO 5, on 14 February 1969. It is the first account of a quasi-parallel (often to be abbreviated q-parallel) shock in the context of the appropriate thermal and flow parameters of the solar wind, using simultaneous data from three statellites and an array of diagnostics including magnetic and electrostatic plasma wave detectors. The report is one of a series describing the structure of the earth's bow shock in detail for each of several identified combinations of β, M and θ_{nB}. The objective of the

series is to document shock structure from a descriptive point of view, using multiple satellite observations and, insofar as possible a reasonably uniform set of multiple diagnostics from case-to-case so that comparisons are facilitated and a common foundation for future theoretical analysis and experimental measurements is established. Other communications in the series cover the turbulent shock (Formisano & Hedgecock, 1973b), the laminar, quasi-perpendicular shock (Greenstadt et al., 1975), and the high β shock (Formisano et al., 1975a).

In the following sections we define the category of shock we observed and the measurements from which the data were obtained. We then describe the data in increasing detail and time resolution, alternating between HEOS 1 and OGO 5, and finally discuss and summarize the results.

CATEGORIZATION

Although it is our intention to categorize each shock type with precision, there is a fundamental ambiguity in attempting to assign a region of parameter space to a shock whose structure is highly irregular and noisy, and this is the basic character of quasi-parallel configurations. Large-amplitude fluctuations make q-parallel normals difficult to define locally, so that θ_{nB} may have meaning at best only with reference to a nominal shock "surface" imagined to exist in place of the complicated wavetrains and particle spectra actually observed. The difficulty may be partially offset by the presence of a distant, unaffected monitor in the solar wind, but even then, extensive upstream effects of the structure may modify the oncoming solar wind so much that velocities, temperatures, temperature ratios and anisotropies, and densities at what we might prefer to call the actual "shock" bear little resemblance to their distant upstream counterparts.

In our case there were some short periods close to or within the interval of interest whose measurements by one or the other satellite we simply took to be the best available representation of the background solar wind plasma. From these measurements we obtained the estimates: $\beta_i = 8\pi NkT_i/B^2 \approx 0.3$; $\beta_{total} = 8\pi Nk(T_i + T_e)/B^2 \approx .6$; $M_A = V_{SW} \cos \theta_{Xn}/C_A \approx 3.7$ and 4.2; $M_{MS} = V_{SW} \cos \theta_{Xn}/(C_A^2+C_S^2)^{1/2} \approx 3.4$ and 3.9, where $C_A = B/(4\pi Nm_i)^{1/2}$, $C_S = (kT_e/m_i)^{1/2}$, and we have assumed $T_e = 1.5 \times 10^{5\circ}K$. The double estimates of Alfvén and magnetosonic mach numbers apply to the positions of HEOS and OGO, which had slightly differing nominal angles $\theta_{Xn} \approx 32^\circ$ and 42°, between solar wind flow and the local shock normals; the first of each pair refers to HEOS 1.

The plasma regime represented here differed, but not severely, from the most common one brought to the earth by the solar wind: the Mach number and thermal-to-field energy ratio were about 20-50 percent and 25-50 percent below average, respectively; not enough to define laminar or cold plasma flow. We deal therefore with a fairly typical, supercritical, warm solar wind. The values estimated place the shock in a category between quasi-laminar and turbulent, according to the scheme of Formisano and Hedgecock (1973a; see also Greenstadt, 1974), because it was supercritical ($M_A \gtrsim 3$), with $\beta_i \lesssim 1$, on the basis of imputed upstream plasma conditions. We reiterate that within the structure, conditions may have differed, probably raising β and lowering M moderately. The mach number might conceivably have become subcritical in the shock structure, and the category have shifted to quasi-turbulent, i.e., $M_A \lesssim 3$, $\beta_i \gtrsim 1$ (Formisano and Hedgecock, 1973a).

The important field-normal angle θ_{nB} was the best-determined parameter upstream (from independent observation by a third satellite) but nonetheless poorly-determined locally, since the field, and presumably the shock "surface," were highly variable. Data could be cited which would reasonably have put θ_{nB} in the range 0 to 20°. Our best overall estimate is $\theta_{nB} \approx 4$ to 10°, so we have placed the shock in the quasi-parallel category, carefully avoiding commitment to the virtually undocumentable term "parallel shock." We emphasize, however, that θ_{nB} was close to zero and that we deal here with borderline parallel geometry.

We think it worth noting that many macroscopic characteristics of q-parallel structure seem, in our experience, to be common to a wide range of M, β combinations, but proof that specific features we describe and inferences we discuss apply to any plasma regime other than that (or those) in which the data were recorded remains to be assembled.

MEASUREMENTS

The data to be discussed here were obtained by the triaxial fluxgate magnetometers of OGO 5 (UCLA) and HEOS 1 (Imperial College), the plasma analyzer of HEOS 1 (Frascati), the JPL plasma analyzer, the TRW plasma wave detector, Lockheed light ion spectrometer (LIS), and UCLA/JPL search coils of OGO 5. The OGO 5 instruments provided high resolution records of the shock at sampling intervals of 1.15 sec/sample, corresponding to a 1 kilobit/sec telemetry rate.

The field and particle instrumentation of OGO 5 and HEOS 1 that provided data for this report are described by Bonetti et al. (1969), Hedgecock (1975), Crook et al. (1969), Snare and Benjamin (1966), Harris and Sharp (1969), and Neugebauer (1970). In using data from the Lockheed spectrometer, we rely here only on relative changes in the raw signature of its energy sweep.

Magnetic field measurements are direct vector recordings of ambient induction, with the HEOS 1 data used to adjust the absolute bias levels of the OGO 5 readings, the latter having been subject to intermittent spacecraft interference. Plasma wave measurements were represented by the field strength in seven channels covering the range 1 to 70 kHz, with most of the shock noise contributed by signals between a few hundred Hz and 2 kHz. Channel center frequencies were at .56, 1.3, 3, 7.35, 14.5, 30, and 70 kHz. Electromagnetic wave noise is represented by the equivalent level of white noise over the bandwidth of each of seven channels of the UCLA/JPL search coils, with center frequencies at 10, 22, 47, 100, 220, 410, and 1000 Hz. The JPL plasma analyzer provided plasma flux readings and upstream velocity and density parameters in the solar wind. The plasma flux was measured by the JPL Faraday cup, which maintained a fixed view toward the sun, with acceptance angle determined by

50 percent transmission at 20° and zero near 40°; absence or decrease of flux usually signifies deflection of flow outside the acceptance angle of the instrument. These quantities were therefore lost once OGO entered the normal sheath. Proton thermalization and diversion of solar wind protons in directions away from that of normal flow were detected by the Lockheed LIS, after the shock was entered, since this instrument looked only in a direction across the solar wind stream. These last measurements are represented here by relative changes in uncalibrated telemetry units.

In addition to the data illustrated in this report, magnetic field parameters for the unshocked solar wind were obtained from the magnetometer of Explorer 35 (NASA/ARC).

GEOMETRIC CONFIGURATION

The geometric and physical contexts in which the observations of 14 February 1969 were made are described by Figure 1. The relationship of the B-X plane containing the HEOS 1 position to the nominal bow shock appears in Figure 1(a) in a conceptual perspective which shows part of the cross section of the shock intersected by the plane. The relationship of the HEOS position to the magnetic shock structure is shown on the B-X cross section in Figure 1(b). For the purpose of illustration, the thickness of the structure is somewhat exaggerated in scale compared to thicknesses inferred directly in this report. The main point of Figure 1(b) is that the spacecraft was situated where $\underset{\sim}{B}$ and $\underset{\sim}{n}$ were nearly parallel. The field varied during the observation interval and OGO was positioned closer to the subsolar point of the shock cross section in its B-X plane than HEOS (see below), but the figure gives a reasonable average view of the geometry that prevailed at both satellites during the encounter with the pulsation structure.

The relative positions of the two spacecraft and the shock are illustrated in Figure 2. Panel 2(a) displays the trajectory segments of HEOS 1 and OGO 5 appropriate to the shock observations, together with sections of shock curves corresponding to the numbered events identified in the next figure. The satellite positions and shock curves are depicted in the rotationally-symmetric X-ρ frame, where $\rho^2 = Y^2 + Z^2$, and shock sections are drawn by simple scale multiplication of the surface $\rho^2 = .331\ [(X - 75.25)^2 - 3686)]$. This surface is a symmetrized version of the average shock described by Fairfield (1971). Both spacecraft were moving outward along their respective orbits during the data interval. The heavy portions of the segments represent the pulsation observations, shortly to be shown.

Panel 2(b) displays the pulsation segments of the two trajectories projected on the Y-Z plane. Dashed and straight lines represent edge-on views of X-ρ and B-X planes through the respective satellite loci. The figure demonstrates that the spacecraft were very close to occupying common X-ρ or B-X planes.

MAGNETIC PROFILE

An overall view of the phenomena described in this report is furnished by Figure 3. The two major panels show the field magnitudes measured by HEOS 1 and OGO 5 magnetometers; one-minute averages in the case of OGO and 48-second samples in the case of HEOS. The three narrow panels at the top show the magnitude and two angles of the interplanetary field $\underset{\sim}{B}_{SW}$ recorded concurrently near the moon by Explorer 35; these are 82-second averages. Note the steadiness of $\underset{\sim}{B}_{SW}$ in contrast with the violent swings in B at the two earth satellites. Indeed, even the direction of $\underset{\sim}{B}_{SW}$ was less variable for this study interval than it usually is.

The two inserts labelled I_p show the behavior of the "binary index" (Greenstadt, 1972b) at the positions of OGO and HEOS, calculated from the field directions measured by Explorer. Values 1 and 0, respectively, are supposed to correpond to q-parallel and q-perpendicular field orientations. We see that shifts between the two levels correspond to changes in orientation of B_{SW} and that the obvious encounters with pulsation shock conditions at both spacecraft occurred while $I_p = 1$. There was a delay for travel time between Explorer and the other vehicles which may have varied during the day; at 0630 it seems to have been about 15 minutes, for the switch from $I_p = 1$ to $I_p = 0$ matched a brief disappearance of upstream waves at OGO and HEOS a short time later. The index is presumably applicable at a given instant only strictly at the "shock," the location of which is unknown almost all of the time, and which appears to be altogether fictitious when the field is locally quasi-parallel.

The numbered times of Figures 2 and 3 call attention to specific events: 1., the first, q-perpendicular crossing by OGO 5; 2., the sudden onset of large

amplitude fluctuations at HEOS 1, obviously a downstream pulsation limit at that instant; 3., the sudden onset of large amplitude fluctuations at OGO, clearly an upstream pulsation limit at that instant, since OGO had already been in the solar wind; 4., the cessation of pulsations and second appearance of solar wind at OGO; 5., the first appearance of solar wind at HEOS.

SHOCK THICKNESS

Figures 2(a) and 4 show the limits on shock location implied by the data of Figure 3: at time 1, the shock was actually at OGO 5, after which it contracted, but moved no closer to the earth than the location of HEOS 1, which was clearly in the magnetosheath at least until time 2, when large amplitude pulsations were first recorded. The brief, unnumbered rise in B at OGO just after 0300 (Figure 3) was a shock encounter which ended at 0314, just five minutes before pulsations began at HEOS (time 2), so the shock was definitely at OGO at that time. At time 2, the shock, or, preferably, the innermost unshocked solar wind was somewhere outside HEOS and inside OGO, the former being in the pulsation region, and the latter in the upstream wave region. At time 3, the outer boundary of the pulsation region moved outward beyond OGO. After time 4, OGO was again in the solar wind, but the shock was still outside of HEOS until time 5, when the shock finally moved inside of HEOS, leaving both satellites in the upstream wave region in the solar wind.

It is immediately apparent from Figure 2(a) that during the simultaneous observations of the large amplitude pulsations, between times 3 and 4, the two satellites did not occupy the same nominal symmetric shock surface. It would follow that the thin shock had been replaced by a "thick pulsation region," for aberrational asymmetry of the shock caused by nonradial solar wind flow cannot place the vehicles on the same nominal shock surface: Figure 4(a) shows two curves representing the nominal shock symmetric about an axis, but tipped away from the X-axis as if in a common plane containing both spacecraft. The 15° tilt of the shock brings the two satellite

positions closer to lying on the same shock surface than does any other tilt angle, but the vehicles are still separated radially by about .5-1 R_E. These data confirm the earlier observations and support the postulate of a thick pulsation region developing under parallel, or quasi-parallel, conditions (Greenstadt et al., 1970a).

The thickness 0.5-1.0 R_E in Figure 4(a) represents an extreme in the least thickness attributable to the shock. A more probable estimate is obtained from Figure 4(b), using the unaberrated, nominal shock profile. The two curve segments marked 3 correspond to the beginning of the common part of the pulsation interval at the respective vehicles; the segments 4 correspond to the end of the common interval. The minimal probable thickness of the quasi-parallel structure, as provided in this configuration by distances 3-3 or 4-4 along the local nominal shock normal, are estimated to have been 2 to 2.5 R_E, depending on how far from the subsolar point the thickness is taken.

PLASMA PROFILE

HEOS 1

The HEOS plasma data afford a view of the general effect of the quasi-parallel shock structure on the solar wind. Figure 5 compares the magnetic profile of the 14 February shock with the plasma parameters derived from the processing scheme of the HEOS 1 plasma analyzer (Bonetti et al., 1969; Formisano et al., 1973). Estimated plasma quantities are, from the top, thermal velocity w, distribution skewness-measure K, density N, and velocity V. Infinite K means a Maxwellian energy distribution; lower K indicates a high-energy tail, at least for a smooth and regular, but skewed, distribution function (Formisano et al., 1973). Each (vertical) set of plasma quantities represents the ensemble of values computed from a single, complete, 384-sec cycle of the analyzer spanning the corresponding time segment.

The most notable property of the plasma during the interval of very disturbed magnetic field was the negligible or at most moderate variation of solar wind velocity. Scanning from right to left, in the direction traveled by the solar wind to the magnetosphere, we see that the outer part of the quasi-parallel "shock" is virtually indistinguishable in the velocity graph. The circled points represent a few velocities observed concurrently by OGO 5, showing the relative constancy of V during the interval and the excellent agreement between the instruments. Only after appreciable penetration of the "shock," at about 0440, did V decrease for more than one cycle at a time, and only after magnetosheath conditions were clearly established

magnetically, at about 0315, did V experience a sharp "permanent" decrease. Moreover, inspection of the individual cycles in the structure (described in a later paragraph) reveals no simple downward shifts in bulk velocity between 0400-0500, but irregular, multimodal spectral distributions whose highest peaks were near the solar wind bulk velocity.

The ambiguity in V at 0529, which corresponded to a sudden spike in B, is probably attributable to a brief encounter with the shock in quasi-perpendicular form. The OGO field data show simultaneously some average direction changes and some brief disappearances of upstream waves suggestive of local changes in obliquity. Unfortunately, the Explorer 35 record suffered a data gap at that time (Figure 3).

In contrast to the velocity, the remaining plasma parameters display clear differences between pulsation and upstream values. The principal properties of these parameters to which we call attention are variability of values accompanying the magnetic pulsations and their clear distinction from those in the solar wind after 0530. We cannot depend on the absolute values between 0310 and 0530 because accurate parameters cannot be obtained, or are not defined, for irregular, multimodal spectra. The plots of these quantities suggest, on balance, a rise in w (temperature) and N and a non-Maxwellian skewing of the ion distribution toward higher energies in the quasi-parallel structure, compared to the solar wind. The suggested effects will be seconded by the descriptions of the next figure. Meanwhile, we require some estimates of absolute values in order to classify the q-parallel observation.

The dashed vertical line marks what appears to have been a density discontinuity in the solar wind. This decrease in N occurred a few minutes after the last large field gradient, so it was probably separate from the pulsation shock structure. The four circled points earlier in the graph, just after 0300, are densities measured in undisturbed solar wind by OGO 5. These values support the inference that the background density had been higher before 0550. However, we note that the second pair of densities from OGO are lower than the first pair, and the time separating them corresponds to a gap during which a magnetic discontinuity occurred, according to Explorer 35 (Figure 3). We think this was a density discontinuity, and we think it reasonable to infer that a band of distinct solar wind plasma, containing the field orientation responsible for the locally q-parallel shock, coincided more or less with the appearance of this structure. The last OGO density, 4 cm^{-3}, is about the same as the low values recorded by HEOS through 0550 and we adopt this as the probable solar wind density during the pulsation interval.

There were fewer data on solar wind temperature than density from OGO, but the three circled points in the topmost panel of Figure 5 indicate a level of T_i comparable to that seen in the ensuing minima and just before 0550 at HEOS. We adopt the last OGO value, 14.4×10^{4}°K as a likely proton temperature in the unaffected solar wind. There is a suggestion that T_i, like N, dropped at the 0550 discontinuity. The estimates of β and M given earlier in the Categorization section were based on the density and temperature figures just discussed.

The apparent net change in the solar wind plasma corresponding to passage through the quasi-parallel structure is supported by examination of averaged spectra, which appear smooth. Figure 6(a) is a graph of three energy distributions superimposed on a common horizontal scale. The ones marked "magnetosheath" and "solar wind" are each averages of several full-cycle spectra obtained by HEOS 1 respectively before 0315 and after 0520 (only when upstream waves were absent in this case). By "average" it is meant that the counts in each energy channel were averaged among the several cycles. Individual spectra contributing to either magnetosheath or solar wind averages were comparatively repetitive and differed little from their corresponding means. The distribution marked "pulsation region" is the average, in the foregoing sense, of all cycles obtained during the two hours or so of pulsation field profile at HEOS. This spectrum clearly shows the plasma energy peak at, or slightly below, the bulk energy of the solar wind but with a lower maximum and a broadened, hotter, more skewed ion distribution. It appears that the ions were severely scattered but the flow was not appreciably retarded by the large amplitude magnetic waves of the parallel structure. This is the same story told by w, K, and V in Figure 5.

Figure 6(b) displays two extremes of the individual pulsation distributions showing two traits typical of all of them: the irregularity below the bulk velocity and the filling-in of the dip between proton and alpha peaks of the solar wind distributions. Most individual distributions resembled either of these or a composite of them.

OGO 5

The upper panels of Figure 7(a) compare the time history of the solar wind flux, when measured by the JPL Faraday cup, with the field magnitude recorded by the UCLA fluxgates. The plotted points are 1-minute averages. Gaps in the flux represent alternate modes of instrument operation. The graphs show the extremely erratic nature of the flux, along with the field, in the quasi-parallel structure between 0350 and 0510. The vertical bars call attention to the apparent inverse relation of F and B: when one is high, the other is correspondingly low.

The lower box, Figure 7(b), is a scatter plot of F against B for the interval 0355-0512. The bars define the high, low, and midrange values of F for each 1γ interval of B. The approximately inverse relationship between the

quantities is clear for values of B ranging between solar wind and magnetosheath levels. The curve in Figure 7(b) is a visual fit of the simple inverse expression $F = 925 \times 10^6/B$, inserted to show how comfortably such a relationship fits the means of the range-bars. Since the response of the cup was substantially linear with respect to off-axis deflections of the solar wind particles, we believe the apparently nonlinear relationship of Figure 7(b) represents a physical characteristic of field and flux behavior, whose true quantitative description will have to be defined in the future by more suitable instrumentation.

The direction of the solar wind flow at OGO was, like the flux itself, highly erratic between 0355 and 0512, and we know from the HEOS data (preceding description) and from occasional measurements of V_{SW} at OGO, that the magnitude of the velocity was not radically altered in the q-parallel structure. We also know that density often rose in the structure at HEOS. The irregular flux profile, especially the minima in flux, were therefore not produced by variations in speed or N but by deflections of the solar wind flow and possibly also by scattering of some of the particle distribution outside the acceptance angles of the instrument (partial transverse thermalization). Such scattering would be consistent with the observed average distributions at HEOS already described. Some, but not all, of the flux decreases were accompanied by the detection of protons by the Lockheed instrument. This will be shown in detail in a later figure.

HIGH RESOLUTION DATA

HEOS 1

The averaged plasma distributions already illustrated serve to demonstrate the existence of a separate category of ion spectra associated with the bow shock's quasi-parallel magnetic profile. They are poor guides, however, to the instantaneous appearance of the plasma over time intervals less than or on the order of a single sampling cycle. The typical period, i.e., peak-to-peak time-interval, of the most conspicuous field fluctuations was near ten seconds, appreciably less than the total HEOS plasma probe cycling time of 384 seconds. Thus, in many cases, individual spectra could not have represented stationary plasma properties.

This aliasing of plasma spectra was anticipated in design of the HEOS 1 analyzer, so that each energy cycle was divided into four 96-second subcycles, each of which covered a wide energy range by sampling every fourth channel. The subcycle feature of the instrument has already been described and used to advantage in an earlier paper (Formisano and Hedgecock, 1973b). In the present report, the subcycle representation of the ion distributions is the only acceptable way of portraying the plasma behavior at high resolution within the pulsation structure at HEOS. It must be remembered, however, that the 96-second subcycle period was also too long to allow accurate depiction of the transient ion distributions in most cases.

The record of field magnitude at HEOS 1 between 0300 and 0600 is shown at the top of Figure 8. Segments of the interval corresponding to representative ion spectral sampling cycles are marked by the lettered and numbered

boxes. The energy distributions of the selected cycles are shown below, with the four component subcycles of each cycle displayed approximately in the actual time sequence in which they were acquired. The two spectra inserted at lower right are average solar wind and magnetosheath distributions. These are repeated in each cycle for comparison with the data actually obtained during the selected cycle. Points at the sampled energies within each subcycle are joined by straight lines.

Cycle A1 occurred entirely in the magnetosheath, apparently when I_p = 0 (Figure 3). The distribution is virtually indistinguishable from that of the average magnetosheath. This example illustrates how steady and reproducible the magnetosheath ion spectrum can be under $I_p = 0$ (quasi-perpendicular) conditions. Cycle A2 spanned a change in plasma regime. The first two subcycles were close to the magnetosheath pattern, while the last two subcycles were a mixture of modified solar wind and magnetosheath patterns. There is no way of knowing in this case whether the sudden transition and drop in field was attributable to crossing of a stationary, or semistationary, boundary between steady magnetosheath and pulsation shock structure or to an encounter with newly-excited pulsation, i.e., quasi-parallel, structure propagating back through the sheath. We favor the latter explanation because of the change of I_p from 0 to 1 at about that time. Cycle A3 was clearly neither magnetosheath nor solar wind, although there was a strong solar wind contribution during the third subcycle. This feature is particularly noteworthy since the high field magnitudes simultaneous with the last half of cycle A3 would seem to have made the presence of solar wind characteristics least probable at that time.

Cycle B, in the midst of the quasi-parallel shock, began during low field readings and ended during high field readings. The distribution, however, was clearly not a simple composite of sheath and wind subcycles. The spectrum was characteristic of neither of these two relatively stationary regimes.

Cycles C1 and 2, also in the midst of the quasi-parallel shock, were likewise neither sheath nor wind. Careful examination of cycles B, C1, and C2 will show that these three distributions were generally similar to each other, despite the rather extreme variations of the field that took place during their acquisition.

Cycle D, still in the pulsation structure, demonstrates the variability of the spectra found there. Again, the distribution was neither sheath nor wind.

Cycle E spanned the change from shock to solar wind. The first two subcycles were very irregular, the third was almost exactly like the customary solar wind, and the last was evidently representative of the shock structure, as in Cycles B and D, despite low concurrent field magnitudes.

The last illustrated distribution, Cycle F, exhibited the type of modification common to solar wind spectra in the presence of upstream waves. The distribution was basically that of the solar wind, with some deviations, particularly in the second subcycle. Recall that the average solar wind spectrum was derived from intervals in which upstream waves were absent.

To summarize the behavior of the plasma ions (protons), on the finest time scale available to the HEOS 1 detector, the particle energy distributions

were irregular and variable within the quasi-parallel shock structure. Nevertheless, a certain similarity among proton spectra was apparent, even when separated from each other in time. These pulsation-associated spectra were definitely not mere time-aliased composites of regular magnetosheath and solar wind distributions.

OGO 5

Wave Polarization. The OGO fluxgate data were transformed into a frame X_{SH}, Y_{SH}, Z_n in which the Z_n-axis contained the least jump during the interval surrounding the abrupt, q-perpendicular shock crossing of 0251 (Figures 3, 10(a)). Thus, the Z_n-component should be aligned approximately with the nominal local shock normal. The X_{SH}-axis was then selected to coincide as closely as possible with the $\underset{\sim}{B}$-vector component in the shock $(X\text{-}Y)_{SH}$ plane. Figure 9 illustrates two sections of field-component data, one in the sheath behind the Q-perpendicular shock, the other in the midst of the Q-parallel structure. The general context of these sections can be seen by reference to Figure 7. We see that most of the small amplitude fluctuation in the sheath was in the Y_{SH}-Z_n plane, and that most of the large amplitude fluctuation of the shock was in the $(X\text{-}Y)_{SH}$ plane. Both sets of oscillations were therefore composed of transverse waves propagating more or less parallel to $\underset{\sim}{B}$, for in the q-parallel structure $\underset{\sim}{B}$ had rotated so as to be nearly parallel to the nominal normal, i.e., the Z_n-axis. We think it likely that the sheath fluctuations are the ion cyclotron waves identified by Fairfield & Behannon (1976) at Mercury. The amplitude of the Z_n-component in the shock is by no means negligible, a circumstance compatible with poorly-defined $\overline{\underset{\sim}{B}}$ and $\underset{\sim}{n}$ when $\Delta B/B$ is so large.

Multiple Diagnostics. Figures 10(a) thru (e) display a number of sections of data as viewed simultaneously by both particle and field instruments of

OGO 5. The sections were chosen to illustrate the full range of forms visible in the OGO record. These are: Figure 10(a), the abrupt, quasi-perpendicular crossing of 0251; Figure 10(b), a gradual transition from high to low average (apparently solar wind) field readings; Figure 10(c), two examples, (i), (iv), of upstream waves directly connected to definite, undisturbed solar wind and two examples, (ii), (iii), of similar waves occurring between sections of pulsations; Figure 10(d), two relatively brief bursts of large amplitude pulsations; and Figure 10(e), two prolonged sojourns in the pulsation structure. In Figures 10(b)-(e), the magnetic X_{SH}-axis is included to represent typical component behavior of the field in the nominal "shock plane."

The abrupt jump from "quiet" magnetosheath to "quiet" solar wind is shown in Figure 10(a) as a reference with which to compare the less familiar quasi-parallel forms of subsequent figures. With the exception of $B_{X_{SH}}$, omitted in (a), the panels are the same for the other figures, (b)-(e). These are, bottom to top: magnitude of B; plasma wave electric noise as sampled sequentially in seven passband channels; proton appearance (in telemetry units), as seen in a direction across the nominal solar wind flow, hence indicating a combination of deflection and thermalization; solar wind proton flux as seen looking toward the sun into the nominal, undeflected solar wind; VLF magnetic noise as sampled by seven channels along one axis of the OGO search coil magnetometer. At the left of the plasma wave panel a typical solar wind spectral signature has been superposed (dotted lines) to mark the contrast between quiet upstream and downstream spectra surrounding a familiar quasi-perpendicular shock crossing; note that the three lowest frequency channels register enhanced noise in the sheath. In the uppermost panel, the measurements of selected

ELF channels have been calibrated and plotted on a common vertical scale, so the relative values seen by various channels can be readily intercompared. Thus a significant enhancement of one channel with respect to the ones adjacent indicates a significant departure from a simple falling spectrum, probably implying the appearance of an ambient signal near centerband of the affected channel. Channel selection from figure to figure represented a compromise between showing important ELF effects and avoiding the confusion of too many overlapping curves.

Several features of Figure 10(a) are important. First, there were sudden changes in average solar wind flux at the shock and in the deflection of protons into the Lockheed instrument. Second, the deflection of particles detected by the LIS was essentially continuous although not constant, in the sheath. Third, thermalization of the protons clearly occurred just behind the ramp. Fourth, the magnetic noise peaked around the shock for all channels with $f \leq 216$ Hz, but showed behavior upstream substantially identical to that downstream, with the most active channel centered at 100 Hz. Although this shock was supercritical and not laminar, the ELF noise followed the same whistler mode pattern seen in the laminar shock (Greenstadt et al., 1975). The large relative separation between the 100 Hz and 216 Hz noise levels resulted from the whistler cutoff at the electron cyclotron frequency along the shock normal. The frequency f_{ci} was about 220 Hz ($B \approx 8\gamma$) in front of the shock and 530 Hz ($B \approx 19\gamma$) behind it, but since θ_{nB} was about 60° in front and 77° behind, $f_{ci} \cos \theta_{nB}$ was approximately 110 Hz both upstream and downstream. As Figure 10(a) shows, frequencies $f < 100$ Hz were enhanced just outside and frequencies $100 \lesssim f \lesssim 216$ Hz just inside the shock, corresponding to detection of rapidly-damped, shock-generated whistlers below the rising f_{ci} in the B-gradient. A more detailed exposition of the ELF phenomenon can be found in the reference cited above.

The contrast between Figures 10(a) and (b) is of considerable interest. Seen by itself, the magnetic field in 10(b), particularly its magnitude profile (2nd panel from the bottom), suggests a "gradual" shock crossing in which the mean field dropped from about 20γ at far left to 10γ or less by 0439, the latter value being close to the interplanetary field. But no other diagnostic supported this view. The solar wind flux, for one, did not return to an average upstream value when the field had been reduced, but showed violent fluctuations including very low flux levels characteristic of the steady magnetosheath (Figure 10(a)). The plasma wave spectrum did not reproduce its typical solar wind format, and the ELF magnetic noise channels showed appreciably more activity at the lower frequencies than they had either in the sheath or the solar wind surrounding the abrupt crossing of Figure 10(a). Conversely, the steady deflection or thermalization of protons associated with the sheath in Figure 10(a) did not appear when B was up to sheath level at 0434. This last observation can be strengthened by reference to Figure 10(e)(ii), which continues Figure 10(b) (to the left): there were nearly two minutes of relatively high average field in which significant thermalization was not apparent. Note that the relatively high and steady field segment surrounding 0438 was accompanied by relatively elevated flux and no evident thermalization. In sum, the quasi-parallel transition from high to low field was grossly different from the quasi-perpendicular case.

The foregoing description leads directly to disclosure of a wholly new phenomenon which for purposes of this report we designate the "interpulsation regime." In an early report on the "pulsation shock" (Greenstadt et al., 1970a,b), attention was called to the appearance of bursts of large amplitude

oscillation, separated by "upstream waves," which appeared almost periodically in the data. The same type of periodic-burst feature occurred in part of the interval we analyze here, but now we are compelled to drop the notion that the bursts are separated by upstream waves. Figure 10(c) depicts two examples of genuine upstream waves (i) and (iv), and two examples of interpulsation waves, (ii) and (iii). The mean field magnitude in all four cases is almost the same, and essentially at the interplanetary field level, while the character of the waves is at least superficially indistinguishable in the magnitude panels. There is a hint of higher frequencies and perhaps slightly larger amplitudes present in (ii) and (iii) than in (i) and (iv), but only by contrast.

The two solar wind segments (i) and (iv) were selected as unquestionably representative of upstream wave trains connected directly to undisturbed interplanetary field, either before or after the waves. The first, in panel c(i), was chosen because it occurred after twenty minutes of upstream waves following a brief exposure to clean solar wind and shortly before the appearance of large amplitude oscillations. Thus this segment should be "deep" in the upstream wave region, near the "shock." The fourth, in panel c(iv), was chosen because the waves were at the edge of the upstream wave region, obviously connected immediately to unperturbed solar wind, as the figure shows. We emphasize that all four of the examples of 8(c) were within the "band" of solar wind we postulated might have been bounded by density discontinuities around 0315 and 0550.

The flux is included in panels c(ii), (iii) for completeness, but little can be inferred from it since it was unfortunately unavailable for intervals

(i) and (iv). We note that the levels are rather low, but it is possible that the incoming solar wind flux may have varied somewhat over the total half-day we are examining, and within any subinterval. Nevertheless, there are extremely low values in (iii) that are hardly compatible with the apparent interplanetary field level they accompany and are lower than the flux values accompanying upstream waves at 0320-0330 in Figure 7(a). A distinction between the pairs of panels appears more readily in the other diagnostics.

Of first interest are the Lockheed data in the fourth panel from the bottom in all four segments. The presence of signal from the light ion spectrometer, with its 12° acceptance angle around the normal to the satellite earth-line, is a much more severe test of extreme particle deflections than the decrease or absence of signal from the Faraday cup, which has a 40° acceptance around the sun-earth line. The test is clearly met behind the q-perpendicular shock of 10(a). In contrast, there was no activity above background in (i) or (iv), nor indeed was there ever such activity at any time during the almost six hours of unambiguous upstream wave residence by OGO on 14 February. Moreover, there is no visible change in the Lockheed record after 0516 in (iv), leaving perturbed and unperturbed sections indistinguishable. In (iii), on the other hand, there was a (barely visible) trace of activity at about the center of the segment, while in (ii) small readings of proton deflection and/or thermalization were constantly present and are evident in the panel. This type of low level, intermittent "cross-flow" proton noise was characteristic of interpulsation segments.

The wave measurements confirm the proton data. The three plasma wave spectra in (i) and (iv) are typical of the solar wind. In fact, no significant alteration of the spectral pattern occurred after the onset of upstream waves in (iv). In contrast, the spectrum of (ii) was moderately altered, particularly in the 1.3 kHz channel, while the spectrum of (iii) departed radically from the solar wind form in the two lowest frequency channels. Similarly, magnetic noise differed between the two pairs of segments: the average noise levels at the lowest frequencies were slightly higher in at least part of the (ii) segment than in either solar wind example, while the ELF noise in (iii) was decidedly enhanced over that in any of the other examples.

To summarize, true solar wind data were similar to each other whether representative of unperturbed solar wind, upstream wave onset, or "deep" upstream wave observation, while interpulsation waves, appearing to emulate upstream waves magnetically, showed diagnostic features suggestive of a quite different regime.

The remaining pair of this group of examples, Figures 10(d) and (e), display the large pulsations themselves, which are the essence of the quasi-parallel structure. Figure 10(d) shows two short bursts of pulsations; Figure 10(e) shows two data segments out of longer intervals of continuous pulsations.

The quasi-periodic character of the large oscillations is striking, particularly in the components, as the illustrated $B_{X_{SH}}$ shows. The full array of diagnostics demonstrates that the pulsation profiles were neither solar wind nor magnetosheath nor alternating samples of these two regimes. The deflection and/or thermalization of the solar wind stream was evident in both the JPL and Lockheed data when the "megapulsations" were present: the flux stream diminished and fluctuated, but protons appeared irregularly across the normal flow in the light ion spectrometer only when the flux essentially disappeared. Electric plasma wave and magnetic ELF wave noise levels were enhanced to values higher than those sustained in the sheath and were comparable to those normally associated with low β, low M, quasi-perpendicular shock crossings. The examples in Figure 10(d) substantiate the distinction in Figure 10(c) between upstream and interpulsation wave regimes by exhibiting, particularly in the ELF wave measurements of 10(d)(ii), little distinction between burst and adjacent data.

DISCUSSION

Magnetic Structure

The distinct character of the pulsation structure of the q-parallel shock has been seen in both magnetic and plasma diagnostics, and the geometry of dual satellite observations here and in an earlier study (Greenstadt et al., 1970a) have implied that the pulsation region can be quite thick. The accidentally similar radial placement of the pairs of satellites in both studies have confirmed the minimal thickness of $\approx 2\ R_E$, but prevented the estimation of any upper limit to the thickness. One additional item is valuable in demonstrating the nature of the extended region occupied by this structure. Figure 11 displays, in a common panel, the sections of pulsation structure recorded simultaneously by OGO 5 and HEOS 1 magnetometers. In this figure, the OGO field measurements have been represented by 48-second samples, simulating the HEOS data to enable a valid comparison between the two separate and dissimilar sampling systems. Attention is directed to the appearance of several segments of time, e.g., 0400-0410, during which $B_{OGO} > B_{HEOS}$. Recall that OGO was the more distant from the earth of the two spacecraft, and it follows that the q-parallel magnetic structure is one in which neither field average nor oscillation amplitudes necessarily decrease with distance outward from the earth. In this case, of course, there could have been lateral dependences of B, and we cannot say what profile would have been recorded along a common normal.

The polarizations of q-parallel pulsations perpendicular to $\underline{B}$, the thickness of the oscillation region, and the seemingly irregular independence of B on distance suggest that the q-parallel magnetic structure may be thought

of as a relaxation of the q-perpendicular shock field jump into large amplitude, transverse waves spreading out along B. A spectrum of frequencies is present which, together with the dispersive quality of local wave propagation, results in a complicated pattern of wave superpositions, sometimes adding to very large field values, sometimes cancelling to nearly zero magnitude.

Plasma Structure

The distinct character of the q-parallel structure has been elucidated in large part by the behavior of the plasma. Perhaps the most serious deficiency in plasma detection on either spacecraft was the inability to obtain accurate directional spectra. Without these it has not been possible to determine just where the protons transferred from the peak to the wings of the solar wind distribution were heading. Since we know that reflected protons of energy more than double the bulk speed are associated with upstream waves, and very likely with the effective viscosity responsible for dissipation in supercritical shocks, it is attractive to infer that the high energy tail of the proton spectra represented particles reflected in one or more magnetic gradients and travelling in directions other than that of the local bulk flow. In a strict sense, however, we have obtained only a one-dimensional view of the plasma, and what we have seen is the "energy" or "speed structure" of the q-parallel shock.

It may reasonably be inferred that almost all previous displays of plasma behavior in the shock have been derived from quasi-perpendicular geometries, whether explicitly so defined or not, since it has been properly customary to disregard data rendered ambiguous by rapid fluctuation over many spectral sampling cycles. Prominent features of various q-

perpendicular shocks have been: a clear reduction of 20-30 percent in V_{SW} (Montgomery et al., 1970); sudden, consistent deflection of solar wind flow (Neugebauer, 1970); rapid proton thermalization with clear appearance of particles transverse to the bulk flow direction (Neugebauer, 1970; Ossakow et al., 1970); and bimodal proton distributions (Montgomery et al., 1970; Formisano and Hedgecock, 1973b). A summary of results can be found in a current review (Greenstadt, 1976), and several of these features are apparent in Figure 10(a) of the present report. Within the limitations of our one-dimensional view, we find that for our q-parallel case the solar wind is slowed down at most only a little, while a significant fraction of the streaming protons are scattered to both higher and lower speeds, in the spacecraft frame. Some of these contribute to a substantial high-energy tail. In addition, we know that the bulk flow is deflected appreciably, often 20° to 40° or more, by individual encounters with large amplitude field pulsations, and that these fluctuations are often not associated with the degree of thermalization that would produce particles normal to the flow. We do not see any indication of a prominent second peak in the proton distributions at 3 to 4 times the bulk energy (Figure 6), but this peak is presumed to be associated with higher mach number (Montgomery et al., 1970; Formisano and Hedgecock; 1973b) than that estimated in our case. If the bimodal distribution can be regarded as the signature of the q-perpendicular structure at high M, then the average, skewed pulsation spectrum (Figure 6) can perhaps be regarded as the signature of the q-parallel structure at low M.

An additional prominent characteristic of the q-perpendicular shock is the flat-topped electron distribution (Montgomery et al., 1970; Scudder et al., 1973). We cannot contrast this directly. There were no electron

data accessible to this study, the London Langmuir probe record being especially difficult to interpret at the 1 kilobit telemetry rate. However, we note that the data from the outbound, apparently quasi-parallel, shock passage by Mariner 10 at Mercury suggest electron density and activity that were different from those associated with either the solar wind or the magnetosheath (Bridge et al., 1974). Such a separate identity would be consistent with the observations by other diagnostics in the present study.

Wave Structure

Electric and magnetic waves appear to have been distinguished in our q-parallel structure by the absence of any outstanding intrinsic values. We note especially that only once did plasma wave noise exceed briefly, 10 mV/m, and rarely did it exceed 2-3 mV/m. This may be contrasted with the almost steady noise at 5-10 mV/m recorded in very high-β shocks (Formisano et al., 1975), and with the very high electric fields in high mach number, q-perpendicular shocks (Greenstadt, 1974). Similarly, the magnetic ELF noise was at lower values than those usually found at elevated β (Greenstadt, 1974). In general, the wave components of the structure were comparable to those associated with simple, laminar, q-perpendicular shocks (Greenstadt et al., 1975). The most interesting wave "structure" was the presence of noise above solar wind background in the interpulsation segments of the data, but the levels of the noise were not striking.

Theoretical Considerations

A comprehensive comparison of observational details with the theory of the microstructure of the quasi-parallel shock is outside the scope of

this report for several reasons, chief among which is that there is neither a single, unified theory nor a small group of competing, easily differentiated models. Those models that have been developed to the point of providing quantitative, or even qualitative, results have been founded on extreme assumptions, e.g., $\beta >> 1$, $\beta << 1$, $M \approx 1$, $\theta_{nB} = 0$, quasilinearity, in order to make the mathematics tractable (Kennel & Sagdeev, 1967; Auer & Völk, 1973). Our case, where $\theta_{nB} \neq 0$, $M \approx 4\text{-}5$, $\beta \lesssim 1$, covers exactly the parameter ranges for which conventional simplifications are inapplicable and for which even approximate solutions or extrapolations of solutions are problematical. There were also experimental difficulties in that the most crucial theoretical quantities governing parallel shock formation, e.g., T_e/T_p, $T_{\|}/T_{\perp}$, were not measured. Without these quantities, especially within the structure itself, validation of theoretical assumptions or predictions cannot proceed. Nevertheless, a few remarks are justified by the nature of the data and by the ideas contained in existing theory.

First, and most importantly, the issue of the existence of parallel conditions in the context of the bow shock must be carefully weighed. The magnetic records displayed here show unmistakably that no identifiable shock could be said to have been propagating instantaneously along $\underset{\sim}{B}$, because every component of the field in the nominal shock-normal frame contained fluctuations whose amplitudes were non-negligible fractions of the total field. Consequently there was no sense in which the upstream plasma flux could have behaved as if it were streaming only parallel to $\underset{\sim}{B}$. We are presently inclined to the view that the incoming solar wind flow, nominally along $\underset{\sim}{n}$ and $\underset{\sim}{B}$, encounters appreciable transient, transverse field before it is "shocked"

and that influential upstream non-parallel effects, which some theories have neglected, must be taken into account in seeking a valid theoretical understanding of the parallel bow shock.

Second, $\underline{B}$, as adopted, was within a few degrees of the nominal normal, probably as close to parallel as experimental techniques can certify, but $\theta_{nB} \neq 0$, and the question can be raised that the observed shock was not strictly parallel, a geometric condition which may have unique, narrowly defined characteristics. However, the bow shock is a three-dimensional curved "surface" and can never be tightly parallel except over a minor fraction of its area. Since theoretical and numerical results have been one-dimensional, it is unknown, given deflected flux, propagating waves, and reflected particles, to what extent the untidy nearly-parallel structure we observed would spread into and destroy any adjacent "clean" parallel structure if it existed. We favor the notion that dimensional effects are important in the bow shock and that locally parallel, unlike perpendicular, average geometry may not be an isolatable state.

Finally, there were some resemblances and dissimilarities of the observations to existing theory that must be noted. The high β, low M calculations of Auer & Völk (1973) developed a genuine shock with a density jump, but the jump was accompanied by an increase in the pressure anisotropy. The enhanced anisotropy would support the firehose instability which would in turn provide a dissipation mechanism and form the parallel shock into a "relaxation" phenomenon with appreciable magnetic turbulence. The authors proposed a qualitative extrapolation to strong (high M) parallel shocks in which they envisioned a double structure consisting of a thin electrostatic

shock ($\Delta X \approx \lambda_D$), distinguished by a density and temperature jump, followed downstream by a broad relaxation structure of the firehose type ($\Delta X \approx 100\ R_i$). They speculated that the magnetosheath itself could be the relaxation zone of the bow shock. In support of this argument, we recall the HEOS plasma measurements of Fig. 5, where the density (and "temperature" as well) appeared commonly to be higher throughout the pulsation interval than it was in what we adopted as the undisturbed solar wind. This result would be consistent with the idea that magnetic turbulence would exist behind an electrostatic shock and within a region of enhanced density. If the density enhancements in the pulsation structure were shock-connected and not merely computer artifacts or interplanetary effects accompanying other, unidentified discontinuities in the observation interval, then the important electrostatic part of the Auer & Völk model might have been responsible.

Are there any measured or inferred quantities of the shock observations of Feb. 14 that can be brought to bear on the Kennel-Sagdeev/Auer-Völk theories? As already noted, none of the most salient quantities was directly measured, let alone measured independently upstream, so we are obliged to reason from rough estimates. The condition on firehose instability is that $\Delta \equiv 1 - 1/2(\beta_e A_e + \beta_i A_i) < 0$, where $A_e = 1 - (T_{e\perp}/T_{e\parallel})$, and $A_i = 1 - (T_{i\perp}/T_{i\parallel})$ (Kennel & Scarf, 1968). The most favorable circumstance for this instability occurs if $A_e = A_i = 1$; i.e., $T_{e\perp} = T_{i\perp} = 0$. If we assume this extreme was the case and take the largest upstream $\beta_i = .3$ and upstream T_e equal to the "connected" average $T_e = 1.56 \times 10^5$°K of Feldman et al. (1973), we get $\Delta = .63 \not< 0$. Realistic estimates of the electron and proton anisotropies make Δ even larger, so there is rough indication that the solar wind was not firehose unstable in the upstream region

outside the q-parallel structure. We are inclined to think that encounter by the solar wind with the large pulsation gradients heated the electrons resistively and made them more isotropic, thus tending to cancel altogether the $\beta_e A_e$ term. If this did occur, then there would have been at most a few instants within the q-parallel structure when $\Delta < 0$ provided we credit the computer-derived values of T_i and assign them entirely to increases in $T_{i||}$.

To the above remarks may be added the observation that, at high resolution, proton (and electron) thermalization and high B tended to occur together, cancelling each other out in the definitions of β_e, β_i and thus acting to keep Δ from going negative. Also, no extraordinary plasma wave (acoustic) noise and no extreme proton heating were encountered at the pulsations. The condition $\Delta < 0$ was therefore improbable on qualitative empirical grounds.

On balance, we cannot rule out the possibility that the firehose instability may have been excited locally at some times, but we do not find direct evidence or persuasive arguments that the electrostatic/firehose relaxation shock model was applicable to the case described in this report in the sense of accounting for the observed overall macrostructure. We suggest that most, if not all, of the quasi-parallel macrostructure we observed was part of a largely upstream, unshocked, or partially shocked plasma state in which the shock relaxed to a thick region with waves, and probably reflected particles, extending far into the upstream medium, and with large amplitude transverse pulses and waves deflecting and

partially thermalizing, through ion waves in their gradients, the incoming solar wind. We propose that separated pulses formed and steepened and that the solar wind streamed through these, emerging as a modified plasma flow corresponding to the interpulsation regime described in the report. The only dissipation mechanisms for which direct evidence was recorded in the region observed were dispersion and ion plasma frequency noise. We speculate that the highest estimated proton temperatures could have been produced by multiple pulsation encounters and anomalous ion-wave resistivity only, and that these were the most likely components of the q-parallel microstructure. The shock appeared superficially as one in which whistlers might have taken the otherwise abrupt transition and run away upstream with it, spreading fragments along the way. This interpretation would be in closest accord with the picture of oblique whistler shocks presented by Tidman & Krall (1971). The upstream conditions in our observed case corresponded to region IV, near the b_x axis, of their Figs. 5.3 and 9.4 and the shock profile corresponded to the forward section including part of the dissipative shock layer, in the sketch of their Fig. 9.5. In addition, we would expect a complex interaction among solar wind particles, reflected protons and electrons, upstream Alfvén waves, and whistlers propagating both upstream and downstream. The picture of Biskamp & Welter (1972) comes to mind, but we lack the diagnostic sophistication for testing their model. We do not exclude two-stream interactions.

SUMMARY

The observed quasi-parallel bow shock structure, at supercritical Mach number and moderate β, was characterized as follows:

1. Irregular, large amplitude, magnetic pulsations, sometimes in bursts, often separated by intervals of smaller amplitude, upstream-like waves;

2. Thickness $\gtrsim 2\ R_E$;

3. Large amplitude, quasiperiodic, transverse magnetic wave components;

4. Solar wind of nominally unreduced, but significantly deflected, streaming velocity;

5. Solar wind of elevated temperature, enhanced density, distinct distribution with skewed high energy tails and irregular low energy envelopes;

6. Inversely related antisolar-directed plasma flux and field magnitudes;

7. Electric and magnetic ELF wave noise comparable to that associated with laminar shocks;

8. Interpulsation regions of upstream magnetic magnitude and wave structure but noisy, deflected, and partially thermalized plasma flow;

9. No direct evidence that the macrostructure was governed by firehose instability as a dissipation mechanism;

10. Macrostructure following the outlines of an oblique whistler shock, modified by additional irregularity and complexity.

ACKNOWLEDGEMENTS

Valuable discussions with R. W. Fredricks and support of NASA Contract NASW-2398 were essential to this study.

REFERENCES

Auer, R. D., and H. J. Völk, Parallel high β shocks and relaxation phenomena, Astrophys. & Space Sci., 22, 243, 1973.

Biskamp, D., and H. Welter, Structure of the earth's bow shock, J. Geophys. Res., 77, 6052, 1972.

Bonetti, A., G. Moreno, S. Cantarano, A. Egidi, R. Marconero, F. Palutan, and G. Pizzella, Solar-wind observations with satellite ESRO-HEOS-1 in December 1968, Nuovo Cimento, Serie X, 64B, 307, 1969.

Crook, G. M., F. L. Scarf, R. W. Fredricks, I. M. Green, and P. Lukas, The OGO 5 plasma wave detector: Instrumentation and in-flight operation, IEEE Trans. Geosci. Electron., GE-7, 120, 1969.

Dobrowolny, M., and V. Formisano, The structure of the earth's bow shock, Rev. Nuovo Cim. 3, 419, 1973.

Fairfield, D. H., Average and unusual locations of the earth's magnetopause and bow shock, J. Geophys. Res., 76, 6700, 1971.

Fairfield, D. H. and K. W. Behannon, Bow shock and magnetosheath waves at Mercury, J. Geophys. Res., 1976, in press.

Fairfield, D. H., and W. C. Feldman, Standing waves at low mach number laminar bow shocks, J. Geophys. Res., 80, 515, 1975.

Feldman, W. C., J. R. Asbridge, S. J. Bame, and M. D. Montgomery, Solar wind heat transport in the vicinity of the earth's bow shock, J. Geophys. Res., 78, 3697, 1973.

Formisano, V., The earth's bow shock fine structure, Correlated Interplanetary and Magnetospheric Observations, VII ESLAB Symposium (Ed. D. E. Page), Reidel, Dordrecht, Holland, 1974.

Formisano, V., G. Moreno, F. Palmiotto, and P. C. Hedgecock, Solar wind interaction with the earth's magnetic field: 1. Magnetosheath, J. Geophys. Res., 78, 3714, 1973.

Formisano, V., and P. C. Hedgecock, Solar wind interaction with the earth's magnetic field, 3. On the earth's bow shock structure, J. Geophys. Res., 78, 3745, 1973a.

Formisano, V., and P. C. Hedgecock, On the structure of the turbulent bow shock, J. Geophys. Res., 78, 6522, 1973b.

Formisano, V., C. T. Russell, J. D. Means, E. W. Greenstadt, F. L. Scarf, and M. Neugebauer, Collisionless shock waves in space: A very high-β structure, J. Geophys. Res., in press, 1975.

Greenstadt, E. W., I. M. Green, G. T. Inouye, D. S. Colburn, J. H. Binsack, and E. F. Lyon, Dual satellite observations of the earth's bow shock, 1. The thick pulsation shock, Cosmic Electrodyn., 1, 160, 1970a.

Greenstadt, E. W., I. M. Green, G. T. Inouye, D. S. Colburn, J. H. Binsack, and E. F. Lyon, Dual satellite observations of the earth's bow shock, 3. Field-determined shock structure, Cosmic Electrodyn., 1, 316, 1970b.

Greenstadt, E. W., Observations of nonuniform structure of the earth's bow shock correlated with interplanetary field orientation, J. Geophys. Res., 77, 1729, 1972a.

Greenstadt, E. W., Binary index for assessing local bow shock obliquity, J. Geophys. Res., 77, 5467, 1972b.

Greenstadt, E. W., Structure of the terrestrial bow shock, Solar Wind Three, Proc. Third Solar Wind Conf., Asilomar (Ed. C. T. Russell), Inst. Geophys. & Planet. Phys., UCLA, 440, 1974

Greenstadt, E. W., Phenomenology of the earth's bow shock system. A summary description of experimental results. Magnetospheric Particles and Fields, Ed. B. M. McCormac, Reidel, Dordrecht, Holland, in press, 1976.

Greenstadt, E. W., C. T. Russell, F. L. Scarf, V. Formisano, and M. Neugebauer, Structure of the quasi-perpendicular, laminar bow shock, J. Geophys. Res., 80, 502, 1975.

Harris, K. K., and G. W. Sharp, OGO 5 ion spectrometer, IEEE Trans. Geosci. Electron., GE-7, 93, 1969.

Hedgecock, P. C., Magnetometer experiments in the european space research organisation's HEOS satellites, Space Sci. Instrumentation, 1, 61, 1975.

Kellogg, P. J., Flow of plasma around the earth, J. Geophys. Res., 67, 3805,. 1962.

Kellogg, P. J., Solitary waves in cold, collisionless plasma, Phys. Fluids, 7, 1555, 1964.

Kennel, C. F., and R. Z. Sagdeev, Collisionless shock waves in high β plasmas, 1., J. Geophys. Res., 72, 3303, 1967.

Kennel, C. F. and F. L. Scarf, Thermal anisotropies and electromagnetic instabilities in the solar wind, J. Geophys. Res., 73, 6149, 1968.

Montgomery, M. D., J. R. Asbridge, and S. J. Bame, Vela 4 plasma observations near the earth's bow shock, J. Geophys. Res., 75, 1217, 1970.

Neugebauer, M., Initial decceleration of solar-wind positive ions in the earth's bow shock, J. Geophys. Res., 75, 717, 1970.

Ogilvie, K. W., J. D. Scudder, R. E. Hartle, G. L. Siscoe, H. S. Bridge, A. J. Lazarus, J. R. Asbridge, S. J. Bame, and C. M. Yeates, Observations of Mercury encounter by the plasma science experiment on Mariner 10, Science, 185, 1974.

Ossakow, S. L., G. W. Sharp, and K. K. Harris, Spectrometer observations in the region near the bow shock on March 12, 1968, J. Geophys. Res., 75, 6024, 1970.

Robson, A. E., Experiments on oblique shock waves, Spec. Publ. 51, ESRO, Frascati, Italy, 159, 1969.

Scudder, J. D., D. L. Lind, and K. W. Ogilvie, Electron observations in the solar wind and magnetosheath, J. Geophys. Res., 78, 6535-6548, 1973.

Snare, R. C., and C. R. Benjamin, Magnetic field instrument for the OGO-E spacecraft, IEEE Trans. Nucl. Sci., NS-13(6), 1966.

Sonett, C. P., D. L. Judge, and J. M. Kelso, Evidence concerning instabilities of the distant geomagnetic field: Pioneer I, J. Geophys. Res., 64, 941, 1959.

Tidman, D. A., and N. A. Krall, Shock Waves in Collisionless Plasmas, John Wiley-Interscience, New York, 1971.

FIGURE CAPTIONS

Figure 1. Context of shock observations of 14 February 1969. (a) Three-dimensional view of HEOS 1 position relative to shock and B-X plane; (b) HEOS location near area of parallel geometry. Distance in earth radii (R_E).

Figure 2. Relative locations of satellite observations and nominal shock curves. Distance scales are in units of earth radii (R_E) in solar ecliptic coordinates. The direction of motion along the trajectory segments marked HEOS 1 and OGO 5 was outward for both spacecraft. The circled numbers in (a) mark nominal shock locations corresponding to the numbered times of Figure 3.

Figure 3. Synoptic magnetic field observations of the quasi-parallel bow shock of 14 February 1969. Explorer 35: 48-sec samples. Pulsation index I_p was computed with $p = 1.6$ (Greenstadt, 1972b). The circled numbers refer to times of boundary crossings or pulsation onsets at either HEOS or OGO.

Figure 4. Basis for estimates of minimal thickness of q-parallel structure. (a) Tipped axis still leaves OGO and HEOS on separate nominal shock surfaces; (b) Shock arcs enclosing trajectory segments corresponding to pulsation data at both satellites define the thickness.

Figure 5. Synoptic plasma and field magnitude data from HEOS 1. Each plasma parameter value corresponds to one complete 384-sec spectrum; the circles represent concurrent values from OGO 5. The double values of V at 0529 represent the range of velocities compatible with an ambiguous spectrum spanning the large 0530, especially between 0314 and 0530, are unreliable, but their general levels relative to the solar wind are significant.

FIGURE CAPTIONS (Cont'd)

Figure 6. (a) Average solar wind, magnetosheath, and pulsation region ion energy spectra from HEOS 1; (b) Two representative pulsation ion spectra.

Figure 7. (a) Comparison of solar wind flux with field magnitude at OGO 5; (b) Apparent inverse relationship between flux and field strength in quasi-parallel structure from 0355 to 0515.

Figure 8. Individual ion spectra (solid lines) from HEOS 1 in original time sequence, displaying the four spectral subcycles in each. The top panel identifies the times and conditions at which the spectra were obtained relative to the q-parallel structural sequence recorded by the HEOS magnetometer. Dashed and dotted lines reproduce the average solar wind and magnetosheath spectra at lower right.

Figure 9. Magnetosheath (left) and pulsation samples of field components measured by OGO 5 (UCLA), showing persistence of preferred wave polarizations normal to $\underset{\sim}{B}$. $\underset{\sim}{B}$ is along $B_{X_{SH}}$ at left, along B_{Z_n} at right.

Figure 10. Multidiagnostic views of various shock conditions seen by OGO 5 on 14 February 69. (a) Quasi-perpendicular crossing.

Figure 10(b). Quasi-parallel field gradient.

Figure 10(c). Two samples (left and right) of upstream wave region and two samples (center) of "interpulsation" wave regions.

Figure 10(d). Two samples of pulsation bursts

Figure 10(e). Two samples of long pulsation trains.

Figure 11. Simultaneous 48-sec samples of quasi-parallel structure seen by HEOS and OGO magnetometers, showing alternation of higher field level at the two spacecraft.

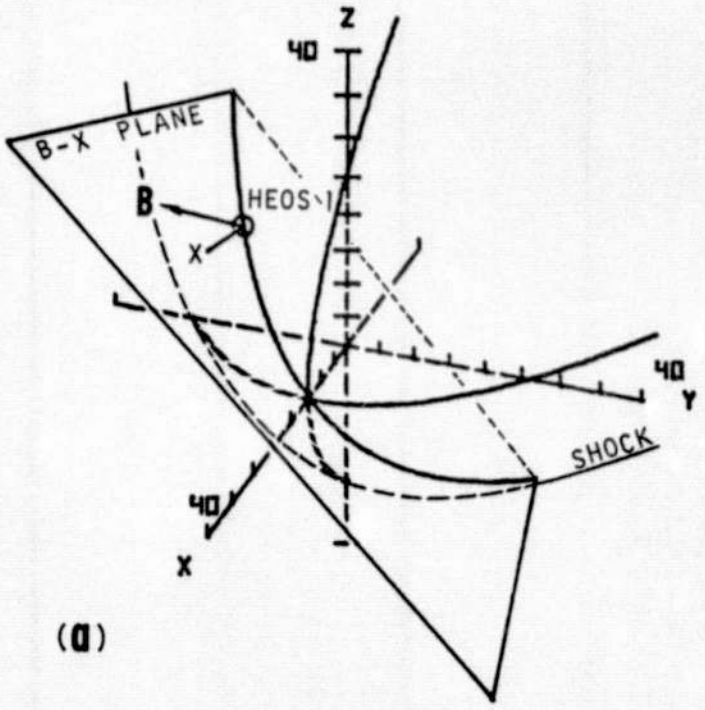

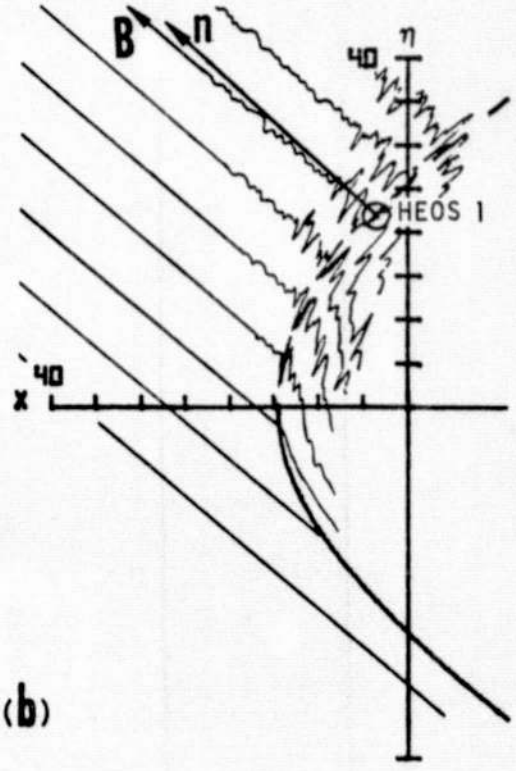

Figure 1. Context of shock observations of 14 February 1969. (a) Three-dimensional view of HEOS 1 position relative to shock and B-X plane; (b) HEOS location near area of parallel geometry. Distance in earth radii (R_E).

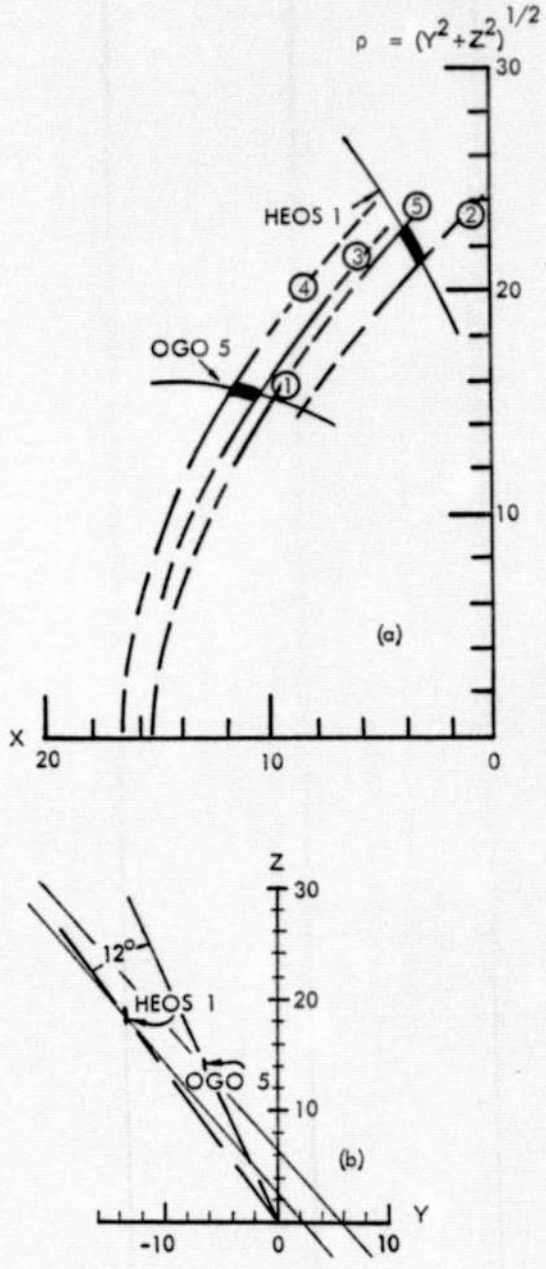

Figure 2. Relative locations of satellite observations and nominal shock curves. Distance scales are in units of earth radii (R_E) in solar ecliptic coordinates. The direction of motion along the trajectory segments marked HEOS 1 and OGO 5 was outward for both spacecraft. The circled numbers in (a) mark nominal shock locations corresponding to the numbered times of Figure 3.

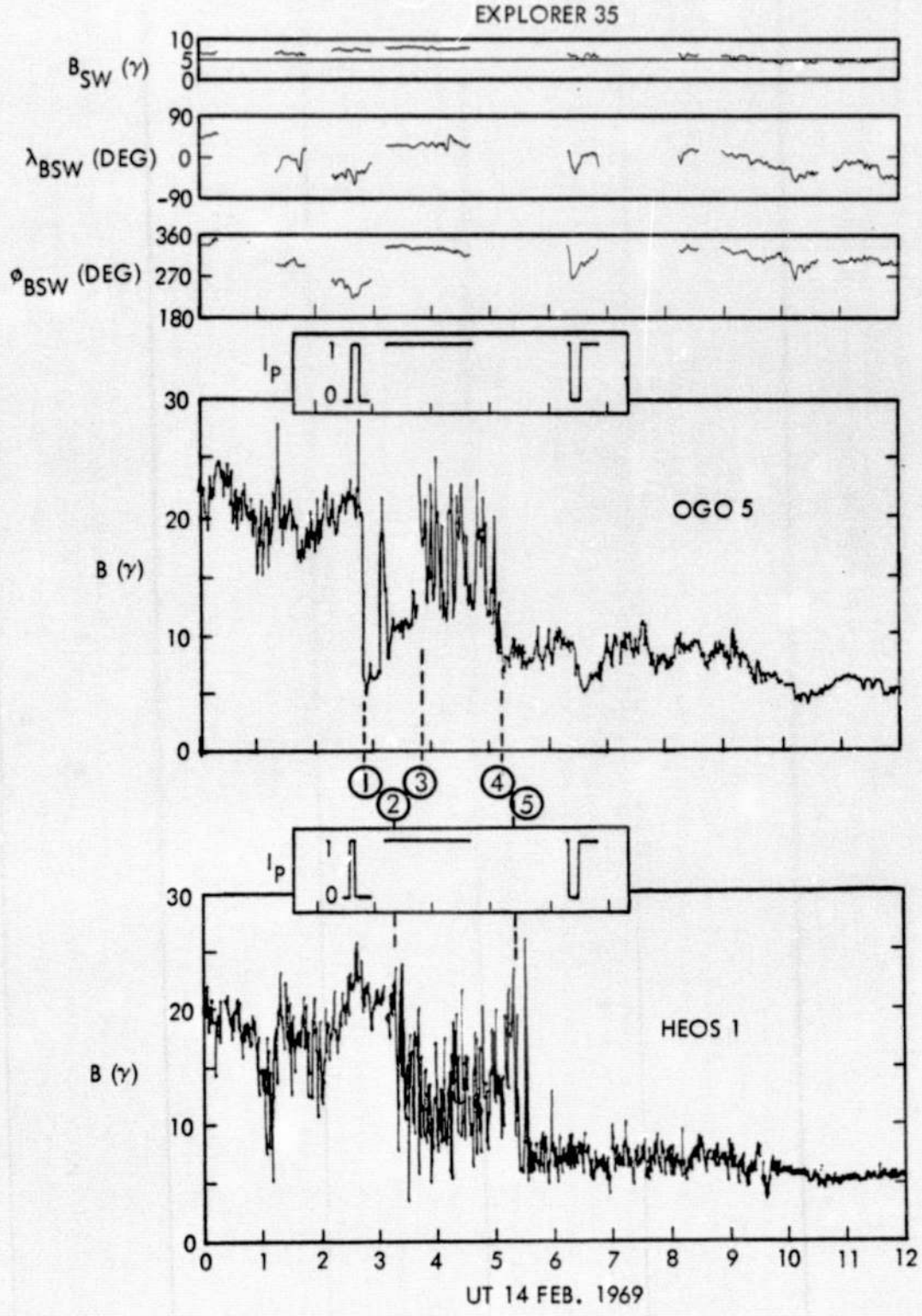

Figure 3. Synoptic magnetic field observations of the quasi-parallel bow shock of 14 February 1969. Explorer 35: 82-sec averages; OGO 5: 60-sec averages; HEOS 1: 48-sec samples. Pulsation index I_p was computed with p = 1.6 (Greenstadt, 1972b). The circled numbers refer to times of boundary crossings or pulsation onsets at either HEOS or OGO.

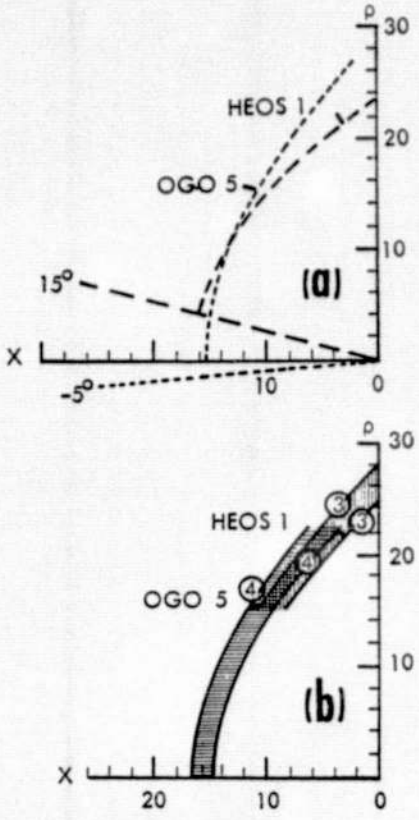

Figure 4. Basis for estimates of minimal thickness of q-parallel structure. (a) Tiped axis still leaves OGO and HEOS on separate nominal shock surfaces; (b) shock arcs enclosing trajectory segments corresponding to pulsation data at both satellites define the thickness.

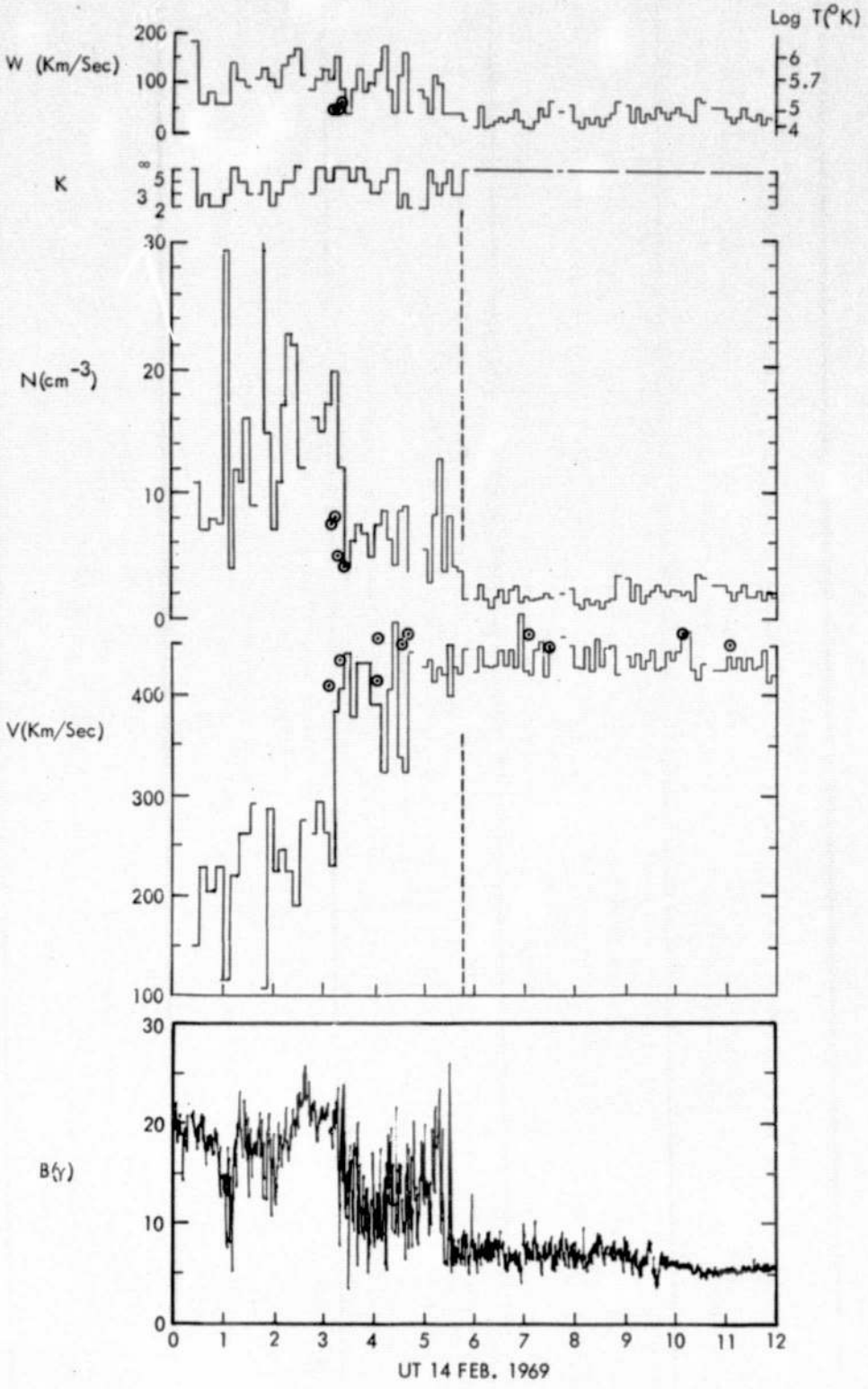

Figure 5. Synoptic plasma and field magnitude data from HEOS 1. Each plasma parameter value corresponds to one complete 384-sec spectrum; the circles represent concurrent values from OGO 5. The double values of V at 0529 represent the range of velocities compatible with an ambiguous spectrum spanning the large 0530, especially between 0314 and 0530, are unreliable, but their general levels relative to the solar wind are significant.

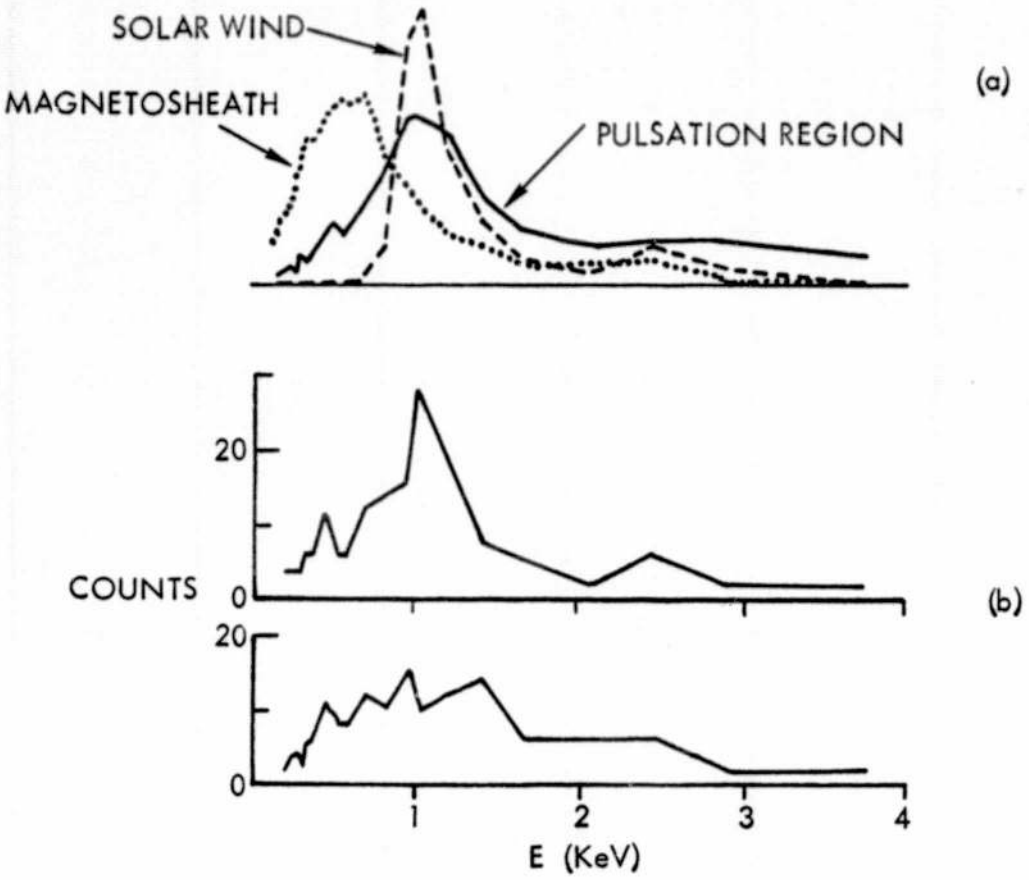

Figure 6. (a) Average solar wind, magnetosheath, and pulsation region ion energy spectra from HEOS 1; (b) two representative pulsation ion spectra.

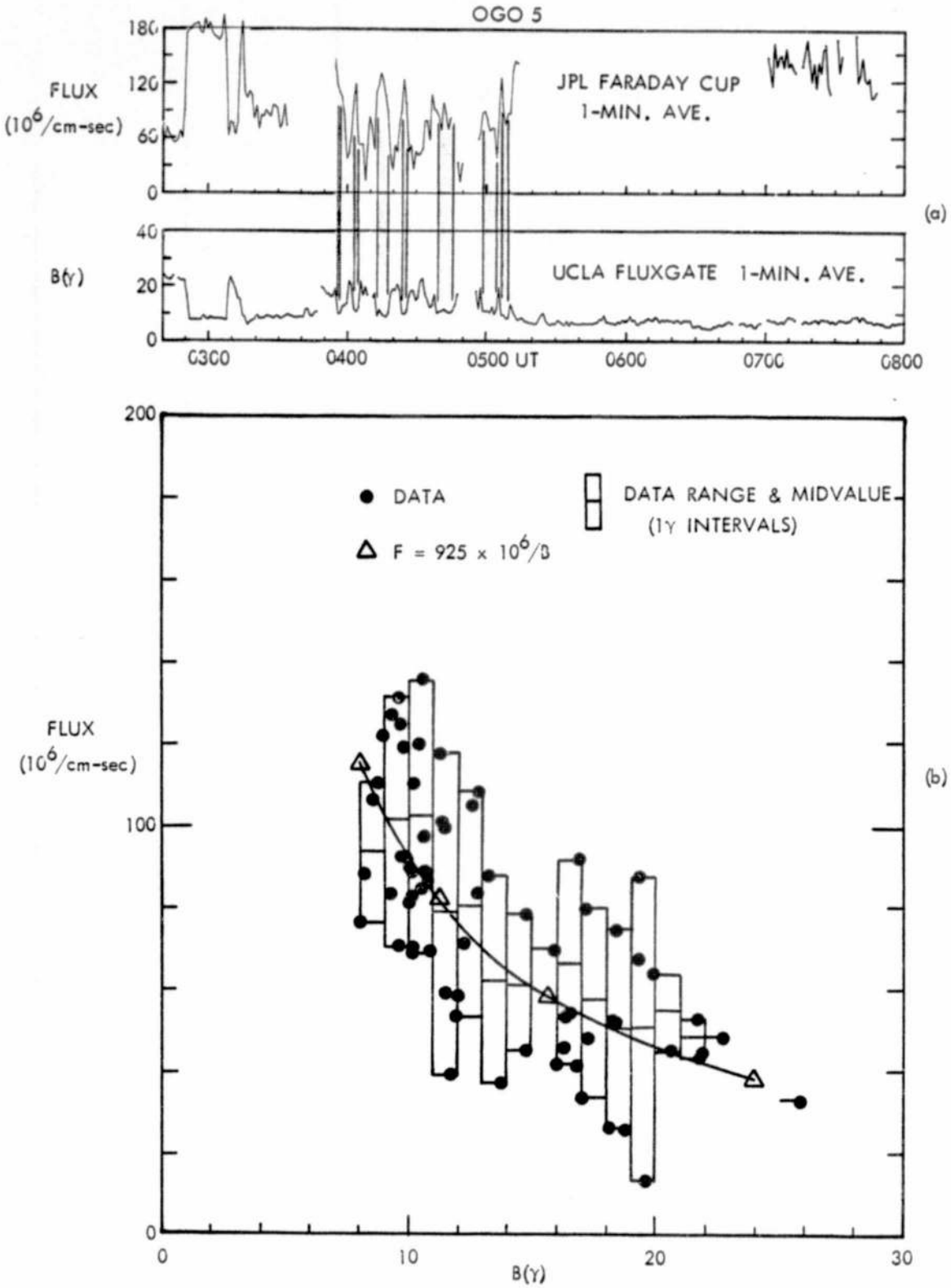

Figure 7. (a) Comparison of solar wind flux with field magnitude at OGO 5; (b) apparent inverse relationship between flux and field strength in quasi-parallel structure from 0355 to 0515.

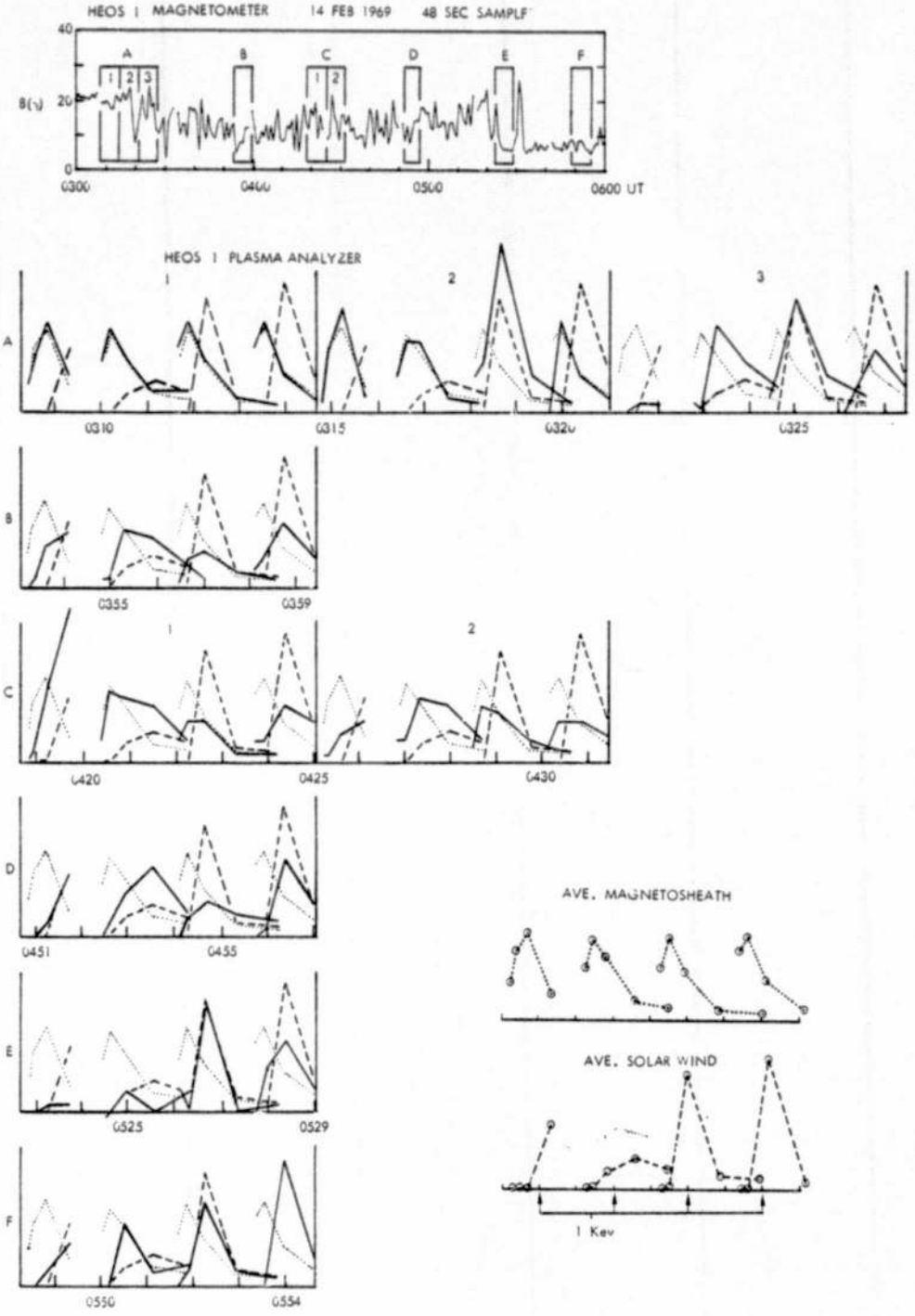

Figure 8. Individual ion spectra (solid lines) from HEOS 1 in original time sequence, displaying the four spectral subcycles in each. The top panel identifies the times and conditions at which the spectra were obtained relative to the q-parallel structural sequence recorded by the HEOS magnetometer. Dashed and dotted lines reproduce the average solar wind and magnetosheath spectra at lower right.

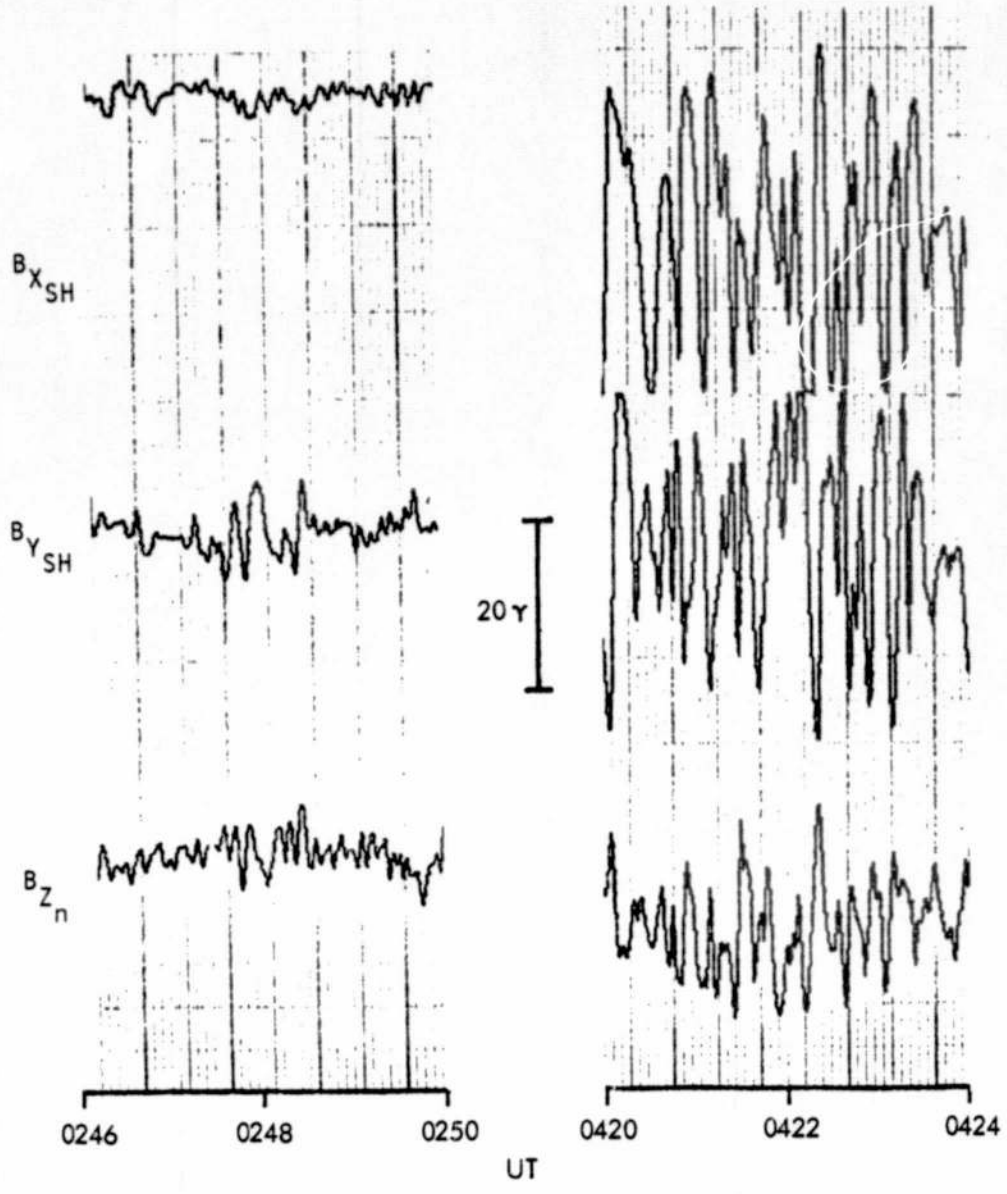

Figure 9. Magnetosheath (left) and pulsation samples of field components measured by OGO 5 (UCLA), showing persistence of preferred wave polarizations normal to $\underset{\sim}{B}$. $\underset{\sim}{B}$ is along $B_{X_{SH}}$ at left, along B_{Z_n} at right.

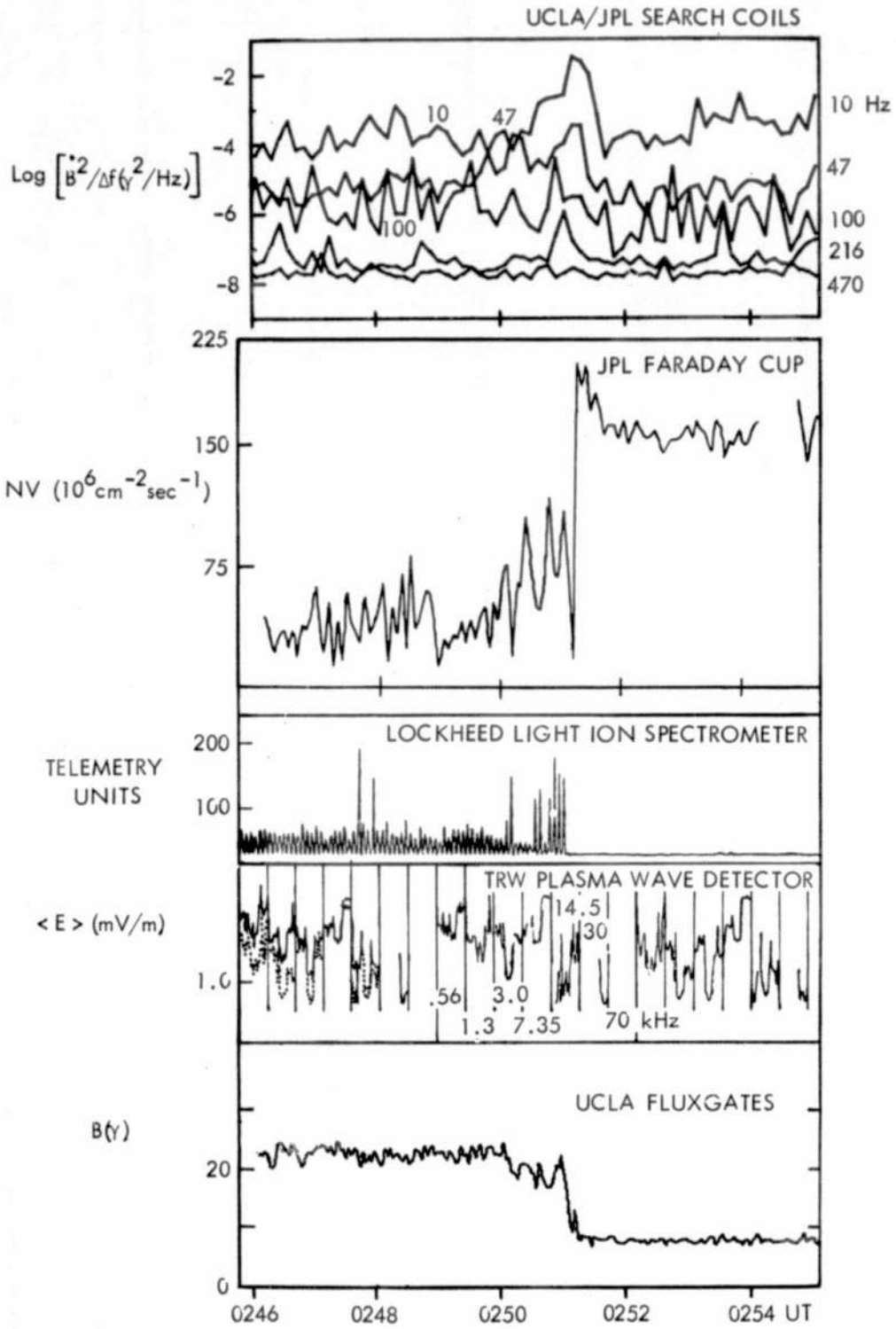

Figure 10. Multidiagnostic views of various shock conditions seen by OGO 5 on 14 February 69.

(a) Quasi-perpendicular crossing.

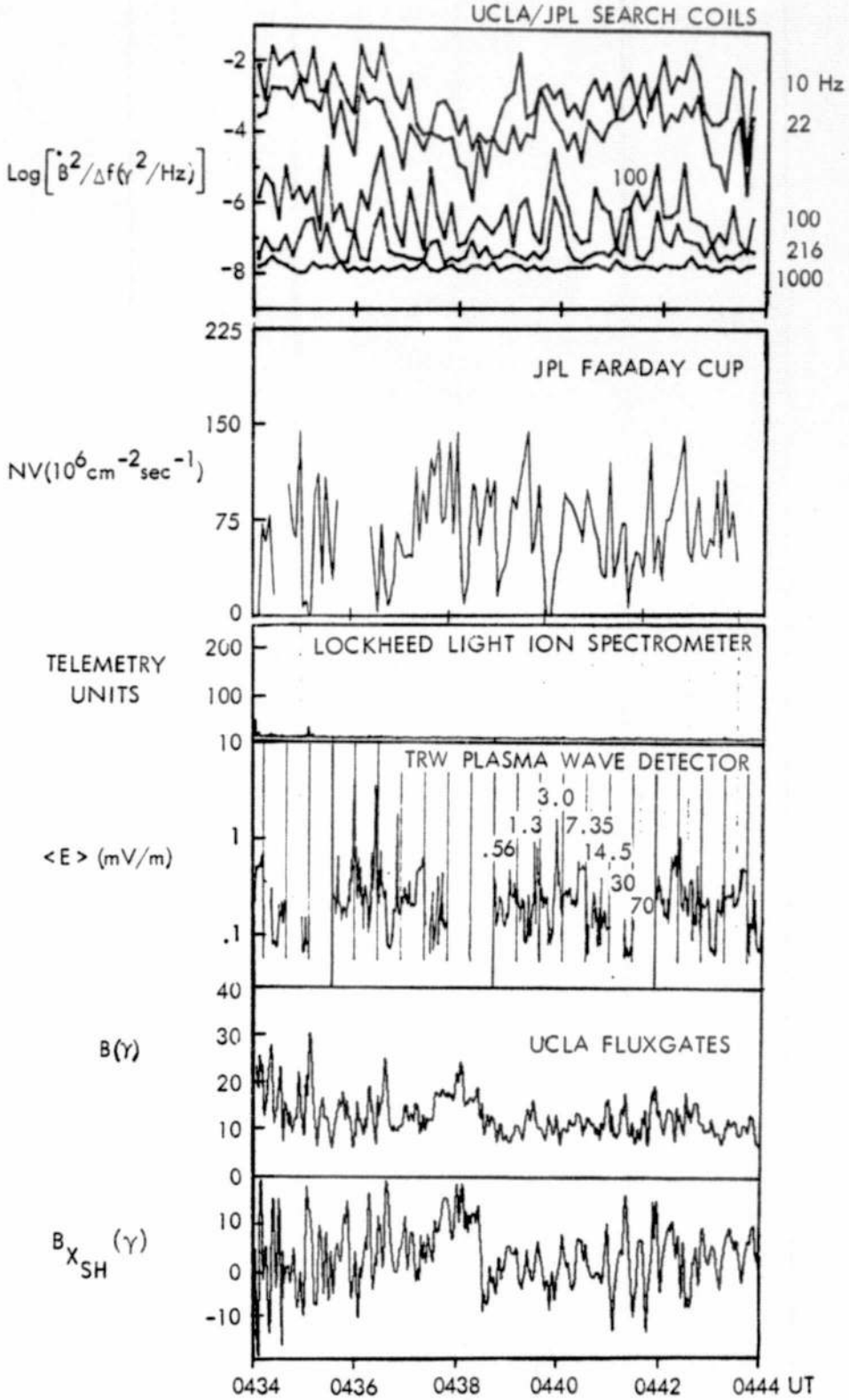

Figure 10(b). Quasi-parallel field gradient.

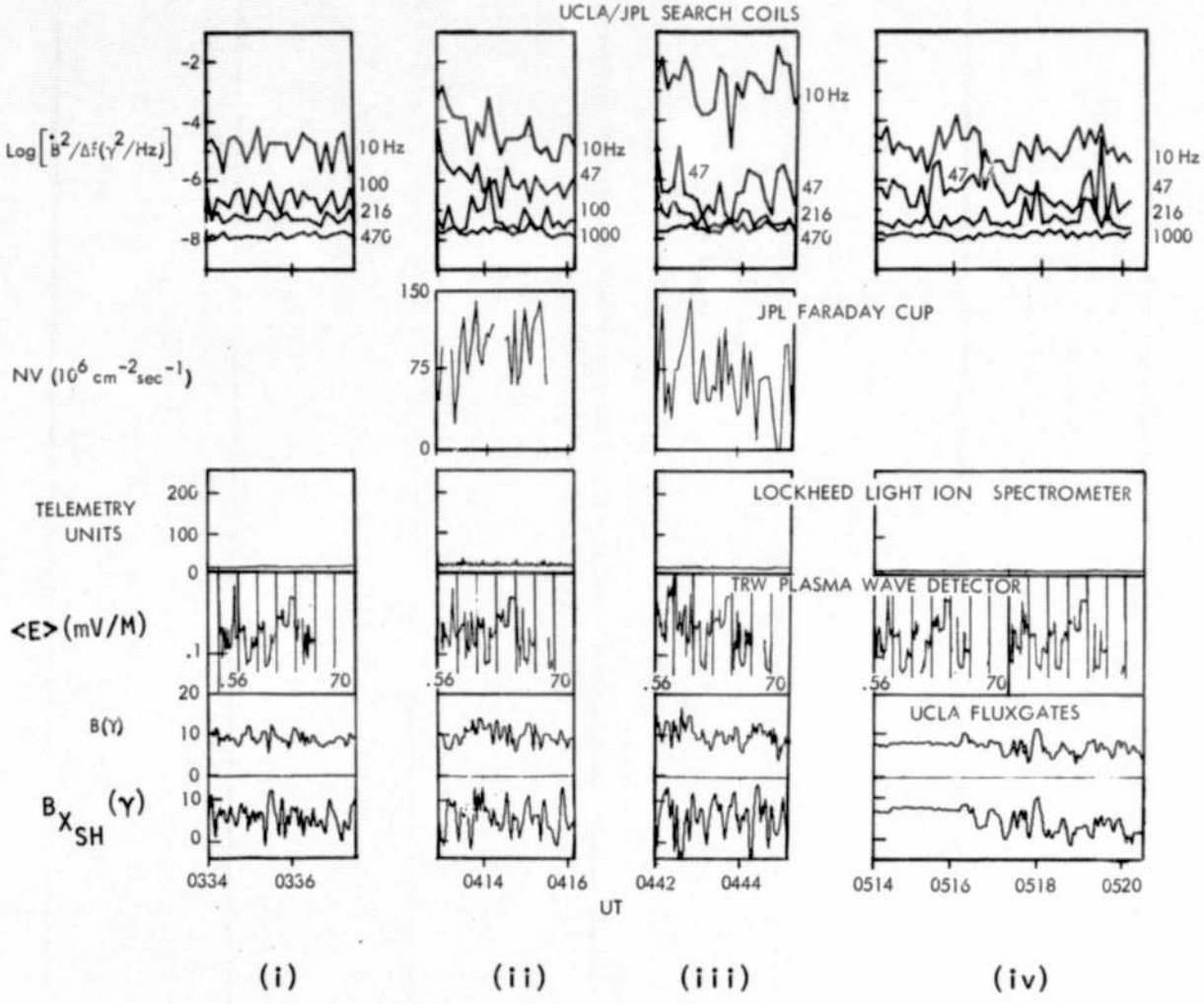

Figure 10(c). Two samples (left and right) of upstream wave region and two samples (center) of "inter-pulsation" wave regions.

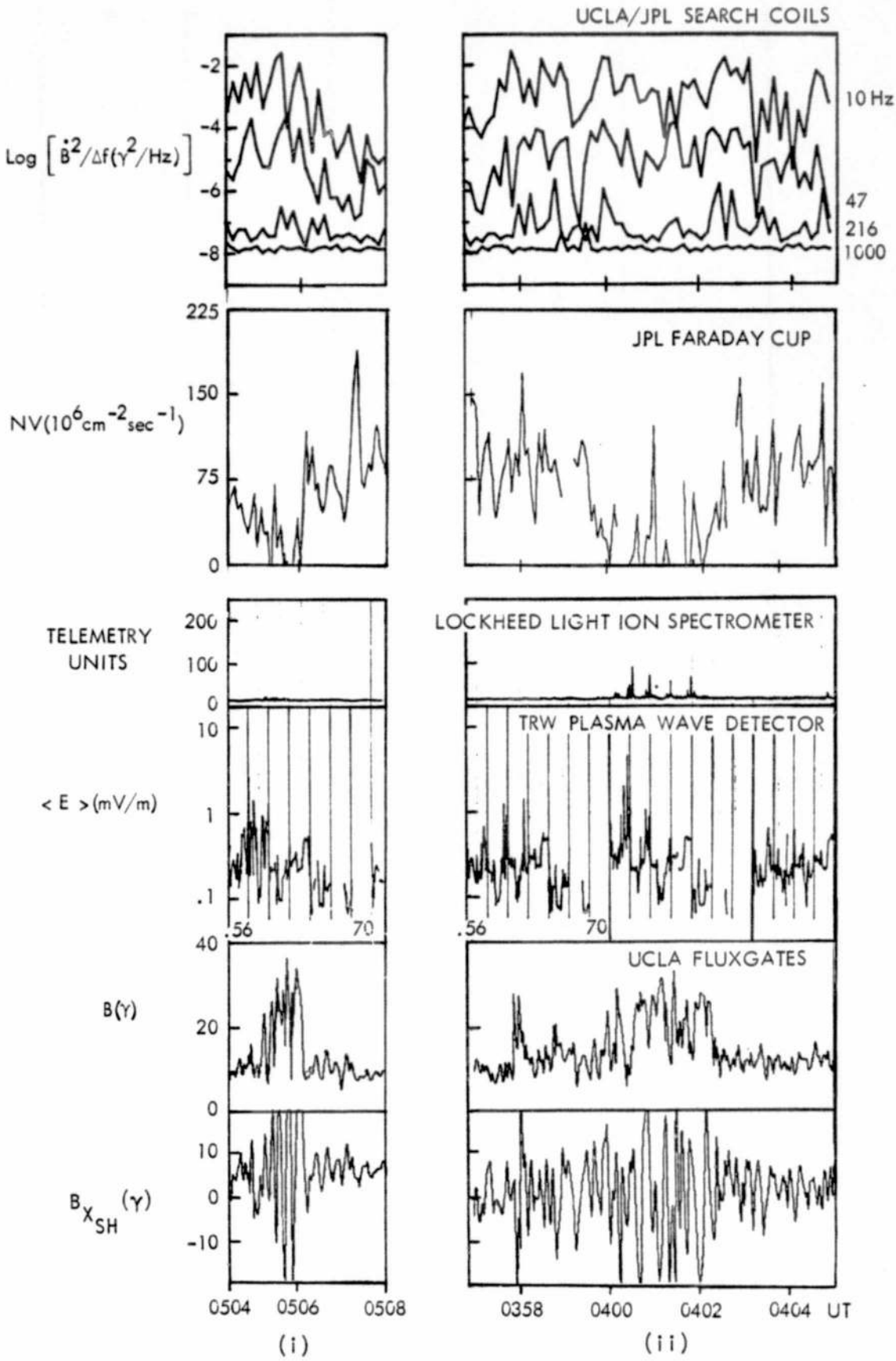

Figure 10(d). Two samples of pulsation bursts.

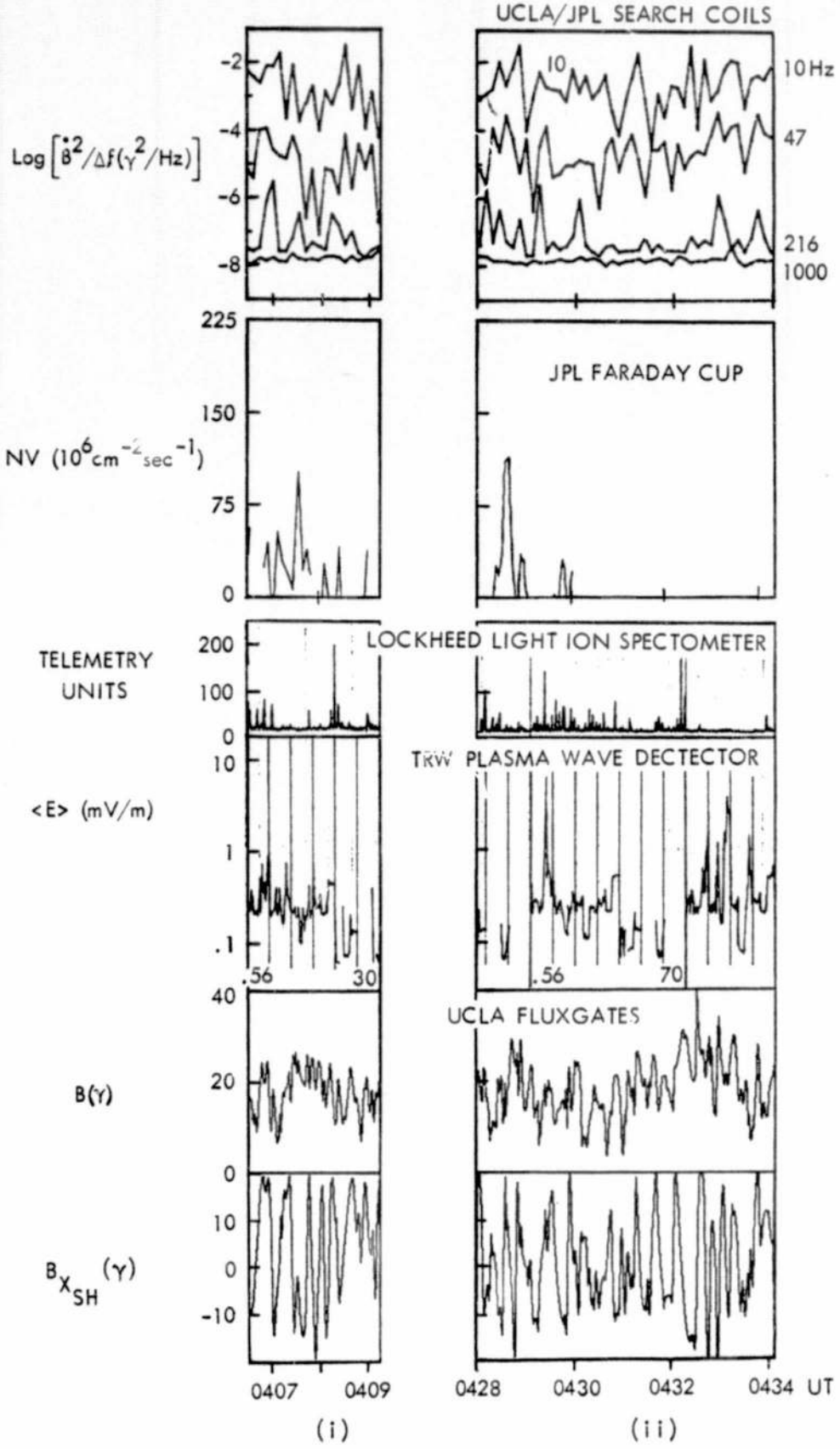

Figure 10(e). Two samples of long pulsation trains.

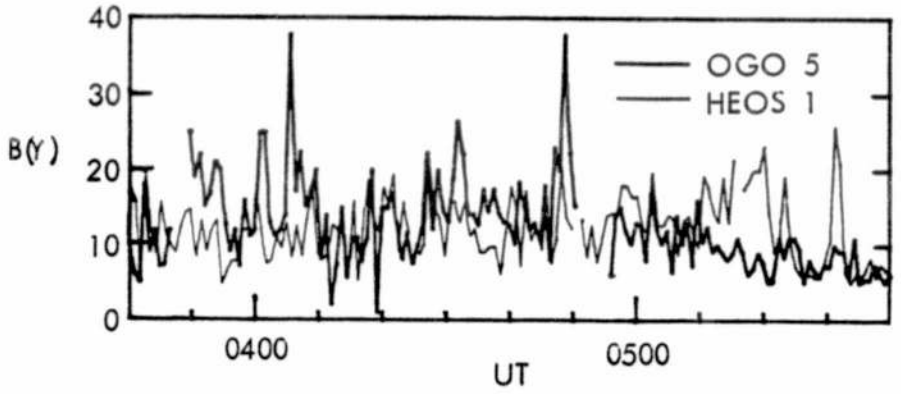

Figure 11. Simultaneous 48-sec samples of quasi-parallel structure seen by HEOS and OGO magnetometers, showing alternation of higher field level at the two spacecraft.